

PHASE B REPORT

on

MATERIALS PROCESSING IN SPACE M512

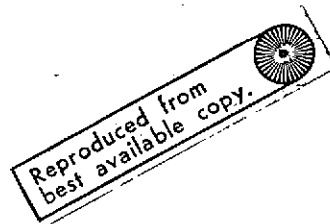
to

GEORGE C. MARSHALL SPACE FLIGHT CENTER
NATIONAL AERONAUTICS AND SPACE ADMINISTRATION
MARSHALL SPACE FLIGHT CENTER, ALABAMA

CONTRACT NAS 8-28725

July 15, 1973

by



H. E. Pattee and R. E. Monroe

(NASA-CR-120266) MATERIALS PROCESSING IN N74-29972
SPACE M512, PHASE B REPORT (Battelle
Columbus Labs., Ohio.) 74 p HC \$6.75

CSCL 11F

Unclas

G3/17 15929

BATTELLE
Columbus Laboratories
505 King Avenue
Columbus, Ohio 43201

ATTENTION

AS NOTED IN THE NTIS ANNOUNCEMENT,
PORTIONS OF THIS REPORT ARE NOT LEGIBLE.
HOWEVER, IT IS THE BEST REPRODUCTION
AVAILABLE FROM THE COPY SENT TO NTIS.

TABLE OF CONTENTS

	<u>Page</u>
INTRODUCTION	1
SUMMARY.	1
SECTION A, EVALUATION OF GROUND CHARACTERIZATION SAMPLES - M551.	A-1
SECTION I, EVALUATION OF GROUND CHARACTERIZATION SAMPLES MCN-2 AND MCN-3 . .	I-1
SECTION II, EVALUATION OF GROUND CHARACTERIZATION SAMPLES MCS-1, MCS-2, AND MCS-3.	II-1

PHASE B REPORT
on
MATERIALS PROCESSING IN SPACE M512
to
GEORGE C. MARSHALL SPACE FLIGHT CENTER
from

BATTELLE
Columbus Laboratories

by
H. E. Pattee and R. E. Monroe

July 15, 1973

INTRODUCTION

This report covers Phase B of a three-phase program entitled "Materials Processing in Space M512". The Battelle effort in metallographic characterization, analysis, and property measurement on ground characterization samples is described. Contractural changes limited this effort to Experiments M551 and M552. This report consists of a summary, two sections on the M552 Phase B studies, and a section on studies completed on M551. The M551 section does not represent the total Phase B effort because of subsequent decisions to process additional ground characterization specimens after the Skylab flight. In general, the individual sections have been prepared to be self contained for future inclusion in final reports. Figure and table notations are selected with this end in mind.

SUMMARY

Phase B effort was divided between experiment M551-Metals Melting and M552-Exothermic Brazing.

M551-Metals Melting

Ten ground base discs were examined to develop the final procedures for the Skylab discs and to provide the data base for future comparison of the effect of zero gravity.

The discs examined are listed below:

<u>Identification</u>	<u>Material</u>	<u>Remarks</u>
2	Stainless Steel	Quadrant Design
B	Stainless Steel	Quadrant Design
P-1	2219 Al	Mo Coating Evaluation
H-1	2219 Al	Final Design
S/N 124	2219 Al	Final Design
S/N 104	Stainless Steel	Final Design
S/N 143	Tantalum	Final Design
S/N 132	2219 Al	Final Design
S/N 107	Stainless Steel	Final Design
S/N 158	Tantalum	Final Design

Sections of Discs H-1, and all of the S/N discs were provided to Marshall Space Flight Center.

All discs were examined visually and by NDT methods. Only x-ray techniques were effective in disclosing subsurfaces features. Dimensions were checked and recorded and out of plane distortion was measured on the last 3 discs. A reference nomenclature system was developed as explained later. A final sectioning plan also was developed. It has been found necessary to make minor adjustments in this plan for individual discs.

M552-Exothermic Brazing

A detailed metallurgical evaluation of two exothermically-brazed nickel and three stainless steel(304L) ground characterization samples was conducted to obtain base-line data for use in determining the effect of weightlessness on the following:

- (1) Wetting and flow of the filler metal
- (2) Solidification of the filler metal
- (3) Metallurgical characteristics of the brazed joints.

Radiography and Visual Examination

Both nickel samples were well-brazed for their entire length. Visual inspection of individual sections from each sample indicated that the joint between the tube and sleeve was almost always completely filled with filler metal. Excess filler metal was puddled at the bottom of the filler metal ring grooves.

All of the stainless steel samples were generally well-brazed for their entire length. However, visual examination of individual sections from each sample confirmed the radiographic indications that there were more void areas in these samples than in those made with nickel. The occurrence of more voids was apparently associated with the slitting of the tube at the center of the sample. As a result, the filler metal flowed from the ring grooves to the sample center, flowed through the slits, and accumulated in a puddle at the bottom inside of the tube.

Metallographic Evaluation

Metallographic studies indicated that the filler metal flowed well and wet the nickel surfaces; the ring grooves were empty except for accumulated filler metal in the bottom. Considerable reaction between the base metal and the molten filler metal occurred during brazing. Products of this reaction formed along the joint interface and became detached as dissolution continued. The width of the reaction zone at the interface was about 0.001 inch.

Metallographic studies of the stainless steel samples indicated excellent wetting of the base metal occurred also. Voids and void areas were present in some areas; these were usually located at the top of the sample relative to its orientation during brazing. Considerable reaction between the base metal and the molten filler metal occurred during brazing. The phase that formed along the joint interface appeared to become detached as dissolution of the base metal progressed and solidified in the filler metal matrix.

Microstructural Studies

Electron microprobe analysis was used to identify the phase constituents of the nickel joint microstructure. The results are indicated below:

- (1) The phase resulting from the reaction of the molten filler metal and the base metal is copper-rich (~95 percent copper).
- (2) The composition of the phase at the interface is similar (or identical) to that of the phase that is distributed between the interfaces.
- (3) The matrix is composed of essentially pure silver.

The microstructures of an exothermically-brazed joint was compared to that of a vacuum-furnaced brazed joint to detect differences associated with the brazing thermal cycle. Base metal-filler metal reactions were more extensive with the exothermically-brazed joints because they were brazed at a much higher temperature than is normally used for furnace brazing with Ag-28 Cu-0.2 Li.

Electron microprobe analysis also was used to identify the phase constituents of the stainless steel joint microstructures.

- (1) A copper-rich phase (73 percent or more copper) formed at the joint interface due to the reaction of the molten filler metal with the base metal.
- (2) This phase was similar or identical to the phase in the matrix.
- (3) The matrix was essentially pure silver.

SECTION A- EVALUATION OF GROUND CHARACTERIZATION SAMPLES - M551

During Phase B the evaluation procedures proposed in Phase A were studied and proven out by examination of ten ground characterization discs. The procedures generally involved visual, nondestructive, and metallographic examinations. The discs examined can be classed in three groups:

- (1) Preliminary- Phase B
- (2) Ground Based- Phase B
- (3) Skylab- Phase C

Only the Preliminary-Phase B group is discussed in this report, since Group 2, Ground Based- Phase B were processed after the Skylab flight. Also, attempts to interpret the data at this stage have been limited because of the uncertainty as to what data may be significant. Instead most information is presented as observations made to date.

MATERIALS

The discs included in the Preliminary- Phase B study are listed below:

<u>Identification</u>	<u>Material</u>	<u>Remarks</u>
2	Stainless Steel	Quadrant Design
B	Stainless Steel	Quadrant Design
P-1	2219 Al	Mo Coating Evaluation
H-1	2219 Al	Final Design
S/N 124	2219 Al	Final Design
S/N 104	Stainless Steel	Final Design
S/N 143	Tantalum	Final Design
S/N 132	2219 Al	Final Design
S/N 107	Stainless Steel	Final Design
S/N 158	Tantalum	Final Design

Procedures

The evaluation procedures proposed in Phase A were studied and applied as required. The visual appearance of the front and back disc surfaces was recorded photographically at 1X. A low power examination using a binocular microscope at magnifications in the range of 7 to 30X also was made. Written descriptions of this visual examination will be prepared for the final Phase B and Phase C specimens.

Radiographic exposures were taken with Norelco-MG-150 equipment on the aluminum and stainless steel and with General Electric - OX250 equipment on the tantalum. The exposure conditions are tabulated below:

<u>Material</u>	<u>Voltage, KVP</u>	<u>Current ma.</u>	<u>Time, min.</u>	<u>Focal Length, inch.</u>	<u>Film Type^(a)</u>
AL	40	5	5	46	M
	47	5	5	46	M
SS	110	5	5	46	AA & M ^{(b)(c)}
Ta	210	8	3	51	AA ^(b)
	250	8	3	51	AA ^(b)

(a) Kodak Designation.

(b) With lead screens

(c) Films exposed together

Generally two exposures were required to provide the proper density for interpretation because of the thickness variation in the disc.

Other non-destructive inspection methods, penetrant and ultrasonics, were not found useful in examination of these discs.

Measurements were taken of the disc thickness with appropriate micrometers, and on some discs dial indicator readings were made to determine the out of plane distortion. The procedure for these later measurements was as follows:

- (1).Set up disc in a lathe chuck and adjust to have the front disc surface perpendicular to the rotation axis.
- (2) Check region near center of disc with dial indicator and readjust as necessary.
- (3) Establish zero reading on center region.
- (4) Record readings at distance of 1/4 inch from weld centerline on either side of weld every 30 degrees.

The discs were marked for sectioning with scribe lines at the appropriate points. The basic pattern for sectioning is shown in Figure A-1. Sectioning was accomplished using a water cooled abrasive wheel, 0.040 inch thick. Sections cut for other investigators were marked and returned to MSFC. The nomenclature used for sectioning and sample designation is listed below:

- (1) 0 degree is target
- (2) Looking at front surface, angle is measured counterclockwise
- (3) All discs are identified with a disc number
- (4) All radial sections are designated by the angle of the plane examined
- (5) All chord sections are designated by the included angle
- (6) All photographs will have a negative number and magnification shown as follows (AAA-20X)
- (7) Direction of view of radial planes will be indicated as, +, looking in direction of weld finish or, -, looking in direction of weld start.

Sections for examination were mounted and polished using conventional metallographic procedures. Sections were examined in both the as polished condition and after etching. The etchants normally used on each base material were as follows:

- (1) Aluminum - $60\text{H}_2\text{O}_2$ - 30HNO_3 -20 Ethyl
Alcohol, 15 drops HF
- (2) Stainless steel - 97HCL , 3HNO_3 -1/2 gram
 CuCl_2
- (3) Tantalum - 30 Lactic,- 40HNO_3 -40HF

All photomicrographs identified as etched were prepared with these etches unless a different etchant is indicated.

Electron probe microanalysis was used as appropriate to identify phases present in the microstructure.

RESULTS

Results of the preliminary Phase B studies are presented in sections containing the data developed on each specimen. The specimens have been grouped by material except for the distortion measurements.

Aluminum Discs

Four aluminum discs were examined. Three of these were of the final disc design and one was a disc used to develop molybdenum coating techniques.

Disc P-1

No defects were noted in the radiograph except crater cracks at the weld stops and dwells. Figure A-2 shows the appearance of this disc as received. The black area is a molybdenum spray coating used for a tracer. A section through the weld zone in the area of the tracer is shown in Figure A-3. No adverse effects of the tracer on the weld region were noted in this section.

Disc H-1

The radiograph showed longitudinal weld cracks near the weld start (125° to 135°), and near the molybdenum tracer (225° to 235°). Cracks in the dwell crater also were apparent. All of these cracks also were visible on the weld surface. Figure A-4 shows the front surface of Disc H-1.

The rectangular cutouts were examined at Battelle. The cross hatch wedge sections were sent to MSFC for examination.

Figures A-5 through A-10 show the appearance and microstructural details in the cut region. Several areas on the cut surfaces indicate the presence of a contaminant or reaction zone. This has probably come from material vaporized from the surface under the weld disc. The very wide cut that resulted in this disc is indicative of an electron-beam power level favoring excessive penetration.

The details shown in Figures A-11 through A-23 are provided for future comparisons of structures and defects. Figures A-24 and A-25 illustrate the technique available to identify phases present in the regions containing the molybdenum tracer.

Disc S/N 124

Figures A-26 through A-32 show the appearance of this disc and selected macro- and microstructures.

Disc S/N 132

Figures A-33 through A-36 show additional features of an aluminum disc.

Stainless Steel Discs

Four stainless steel discs were examined. Two were of an early quadrant design and the last two of the final designs.

Disc 2 and Disc B

Figures A-37 through A-39 show the front and back surfaces of Disc B and Disc 2. The quadrant thickness of these discs is tabulated below:

<u>Region</u>	<u>Thickness, inch</u>	
	<u>"B"</u>	<u>"2"</u>
Cut	0.027	0.026
Full penetration	0.097	0.049
Partial penetration	0.168	0.123
Dwell	0.258	0.248

A large number (about fifty) macro and microphotographs were taken of sections from these discs. They are available, but not shown herein because of later changes in material and disc design.

Disc S/N 104

Figures A-40 through A-50 show the front surface and transverse sections through the various regions of a stainless steel disc.

Disc S/N 107

Figures A-51 through A-54 show additional features of a stainless steel disc.

Tantalum Discs

Two tantalum discs, both of the final design, were examined.

Disc S/N 143

This disc is shown in Figure A-55. Sectioning was limited by the extensive cutting that occurred. Figures A-56 through A-63 show the sections examined.

Disc S/N 158

Figures A-64 through A-68 show features of this disc and selected sections taken.

Distortion Measurements

The distortion measurements are given in Table A-1. Distortion in the cut region was greater than in other regions.

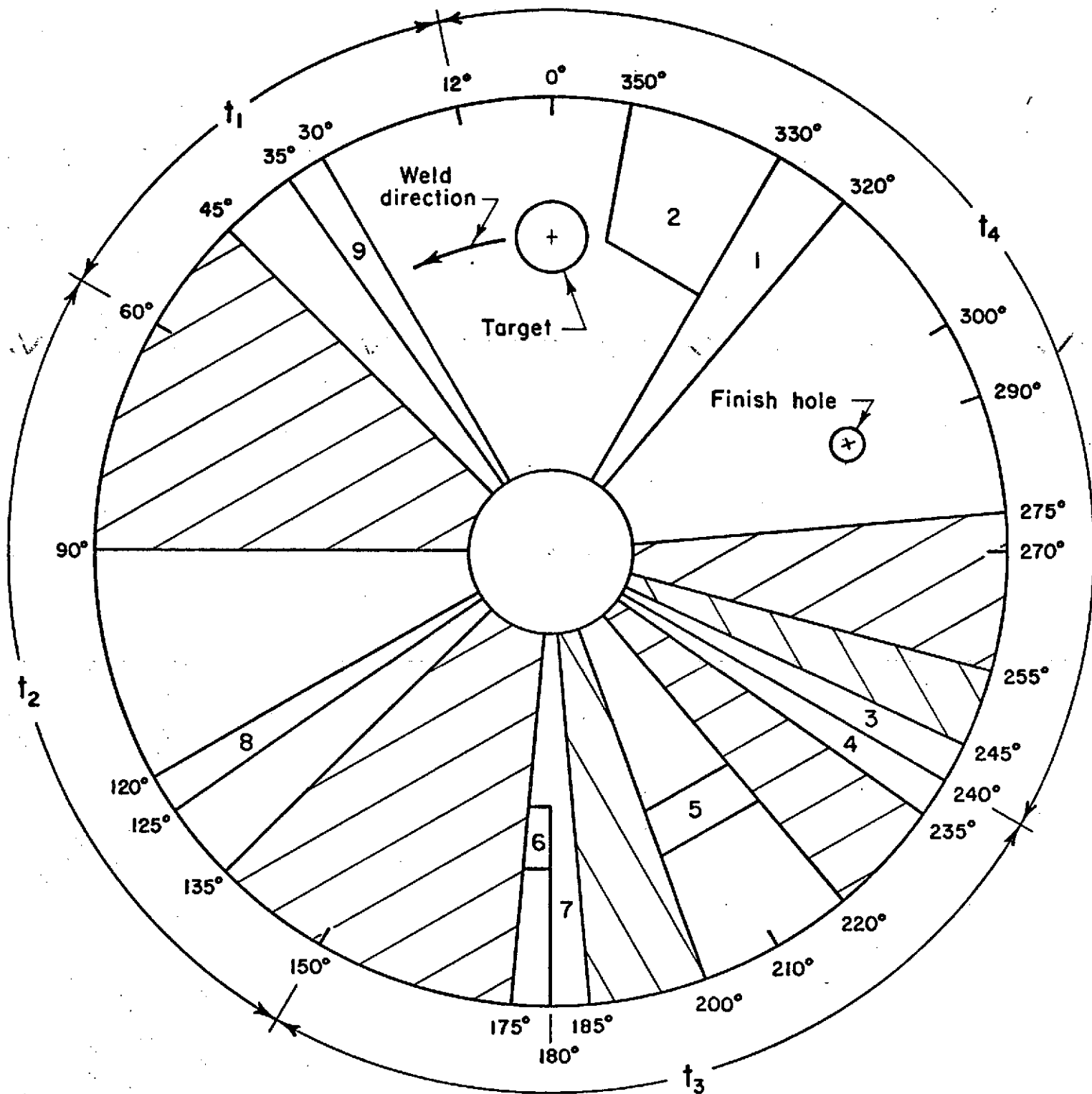


FIGURE A-1. SECTIONING PLAN - M551

Numbered Sections - BCL



- MSFC



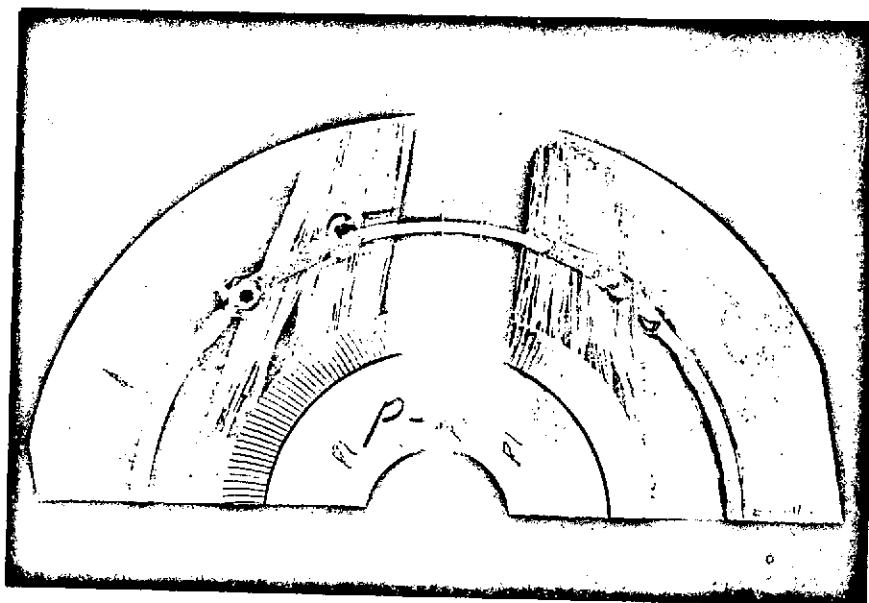
- UK

T₁ - Cut

T₂ - Ramp

T₃ - Full penetration

T₄ - Partial penetration/dwell



2G905-0.5X

FIGURE A-2. FRONT SURFACE OF P-1



Etched

5G265-20X

FIGURE A-3. SECTION P-1 AT TRACER REGION

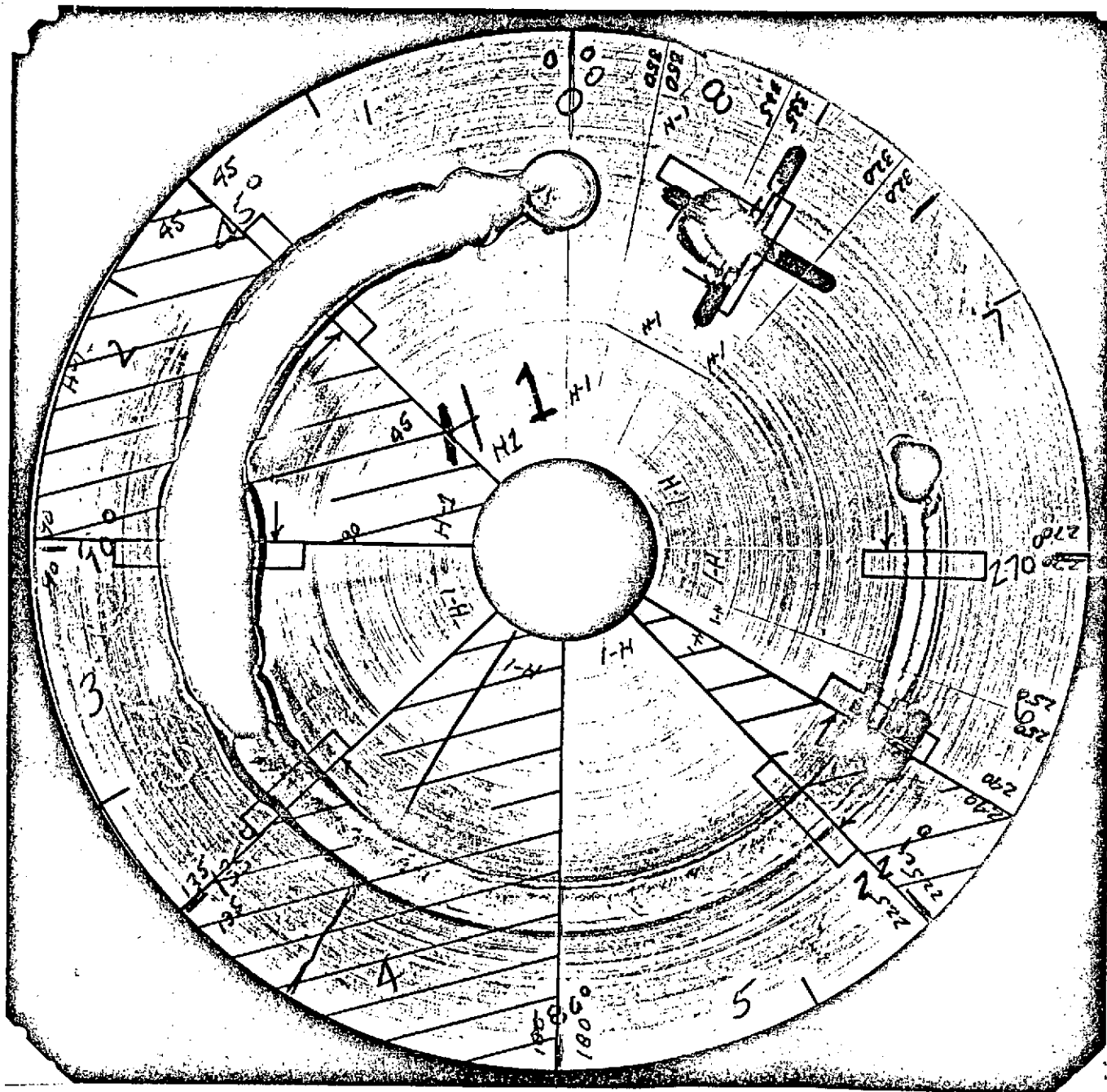
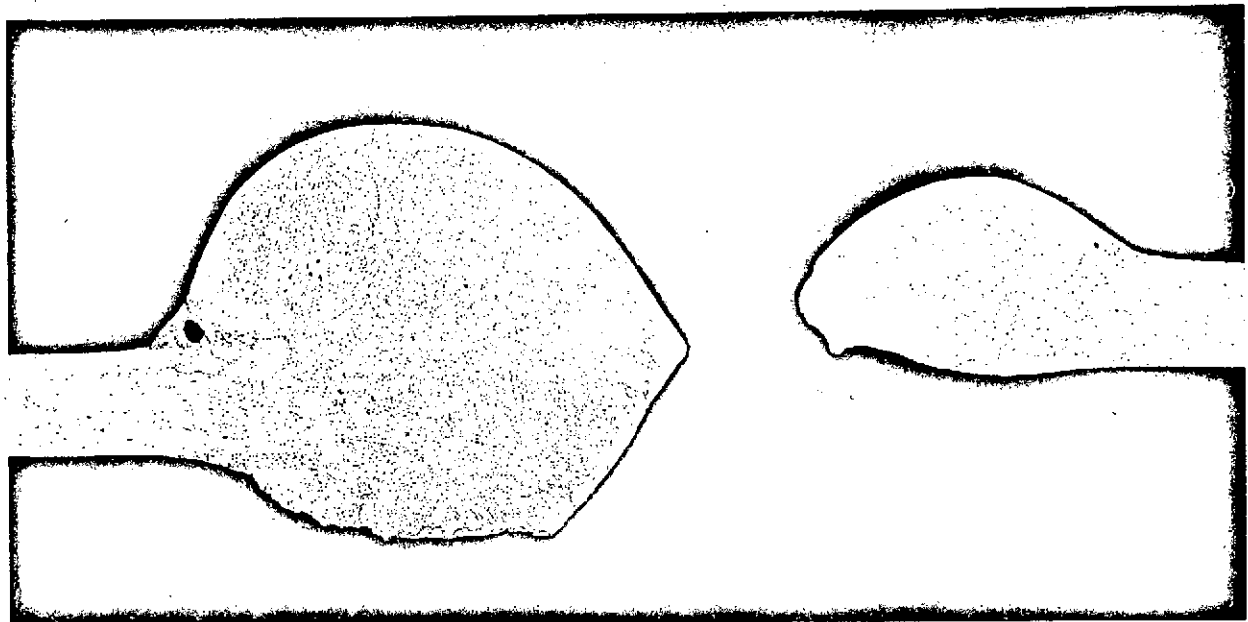


FIGURE A-4. FRONT SURFACE H-1

2G906-1X

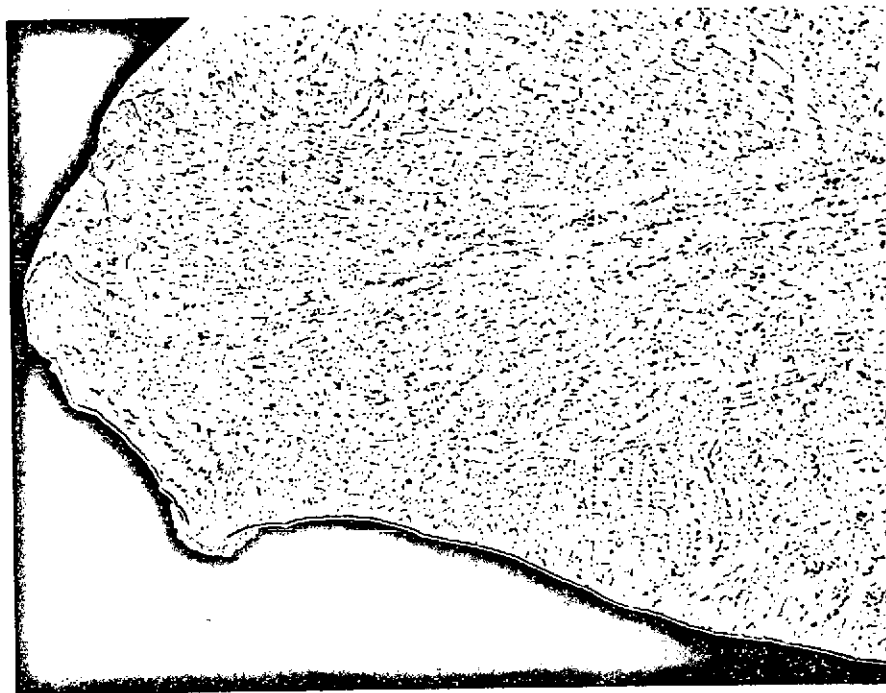


45°(-)

Etched

5G264-20X

FIGURE A-5. SECTION THROUGH CUT REGION -H-1

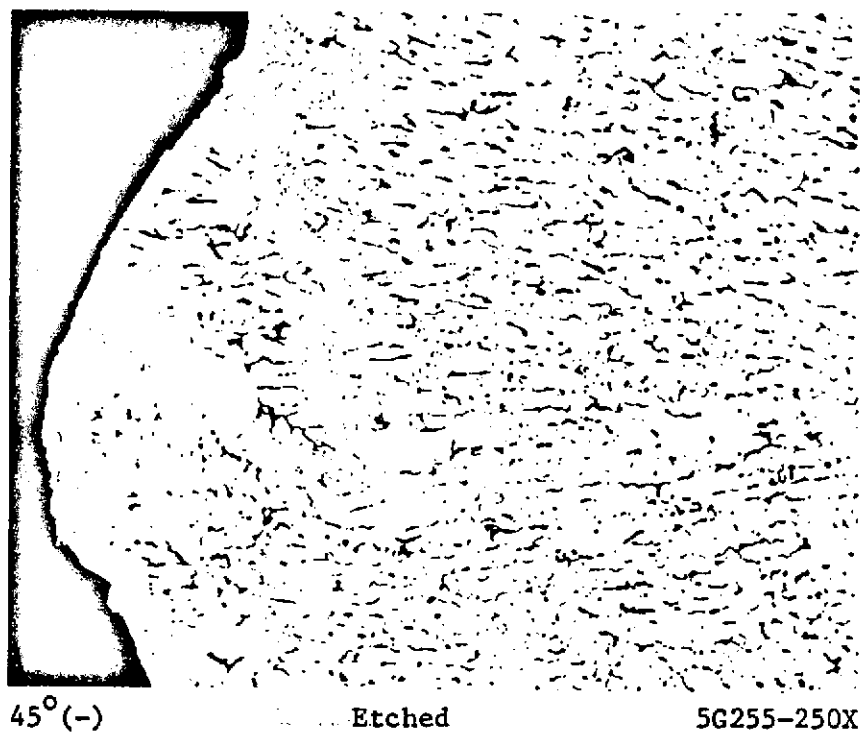


45°(-)

Etched

5G254-100X

FIGURE A-6. SURFACE OF CUT ON INSIDE -H-1

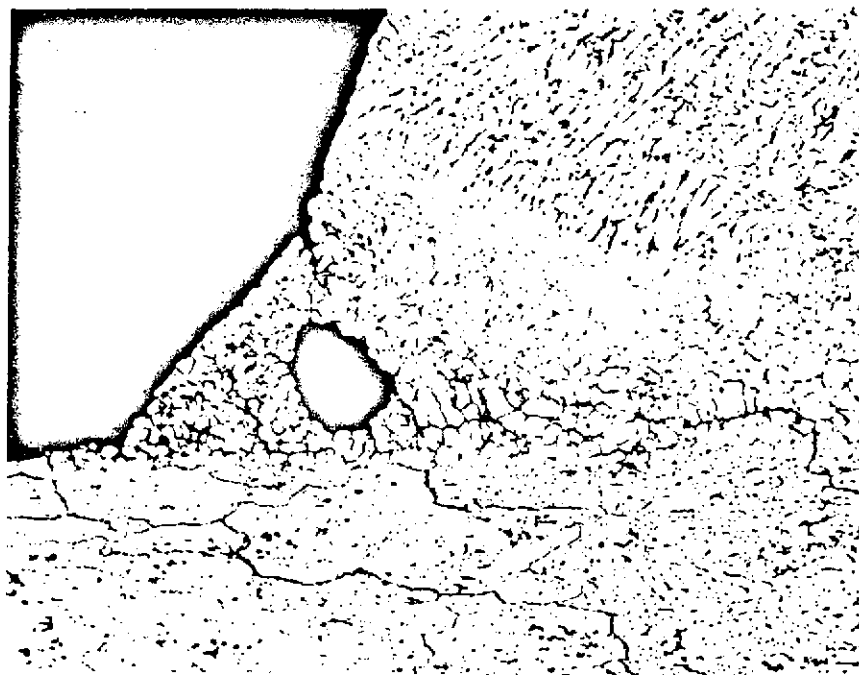


a. Enlarged area of Figure A-6



b. Bottom surface of cut on outside

FIGURE A-7. SURFACE OF CUT -H-1

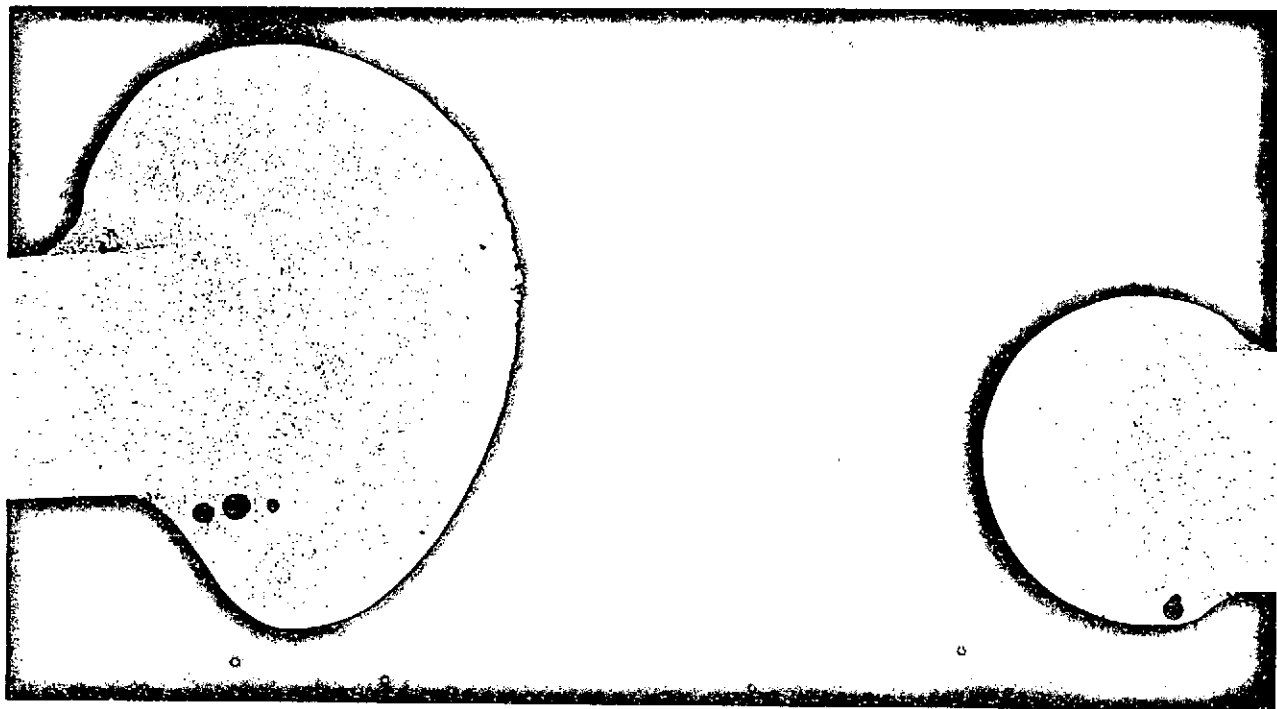


45°(-)

Etched

5G253-100X

FIGURE A-8. PORE IN SECTION AT BASE METAL INTERFACE
H-1



90°(+)

Etched

5G263-20X

FIGURE A-9. SECTION THROUGH RAMP REGION -H-1

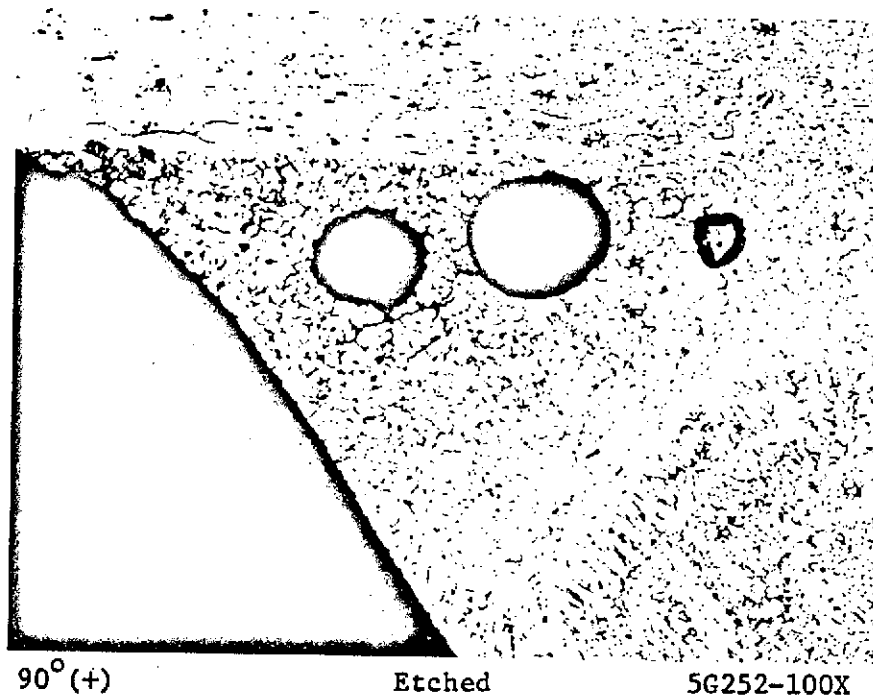


FIGURE A-10. PORES IN RAMP SECTION -H-1

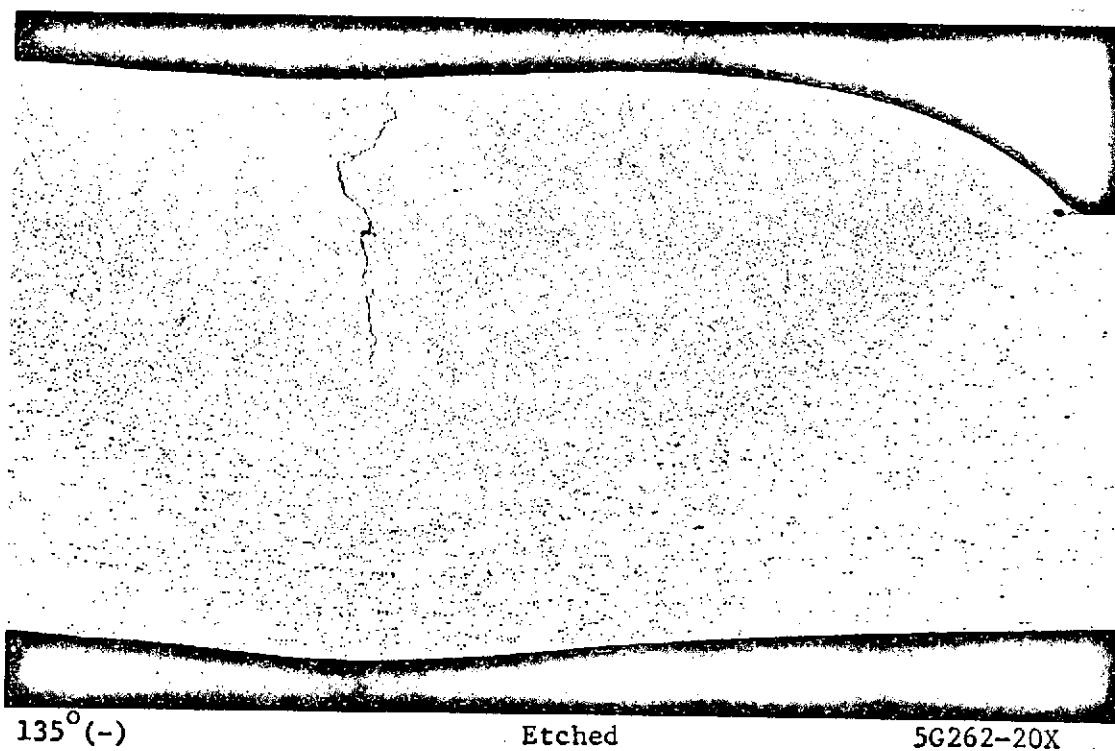
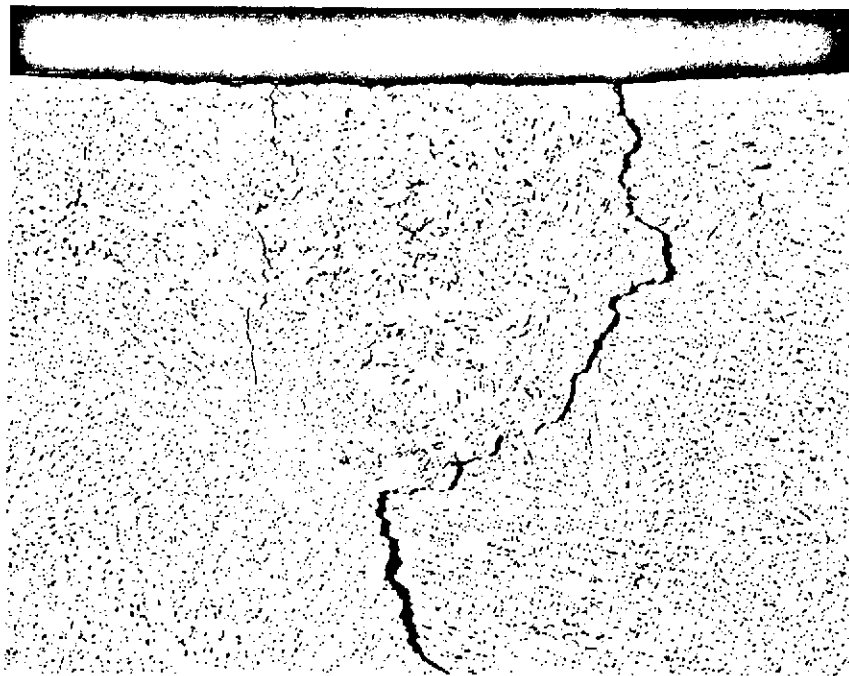


FIGURE A-11. SECTION THROUGH CRACK NEAR WELD START



135°(-)

Etched

5G250-100X

FIGURE A-12. ENLARGEMENT OF LONGITUDINAL CRACK
AT WELD START - H-1

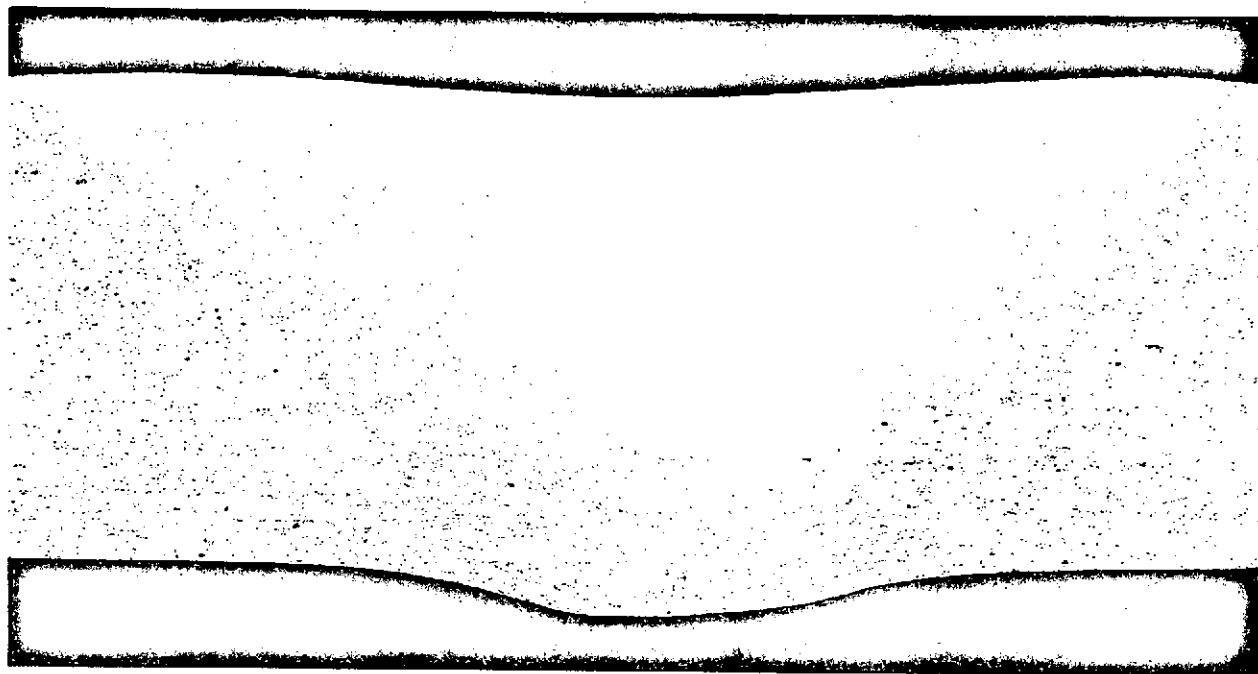


135°(-)

Etched

5G251-500X

FIGURE A-13. PORE AT INSIDE EDGE OF WELD - H-1

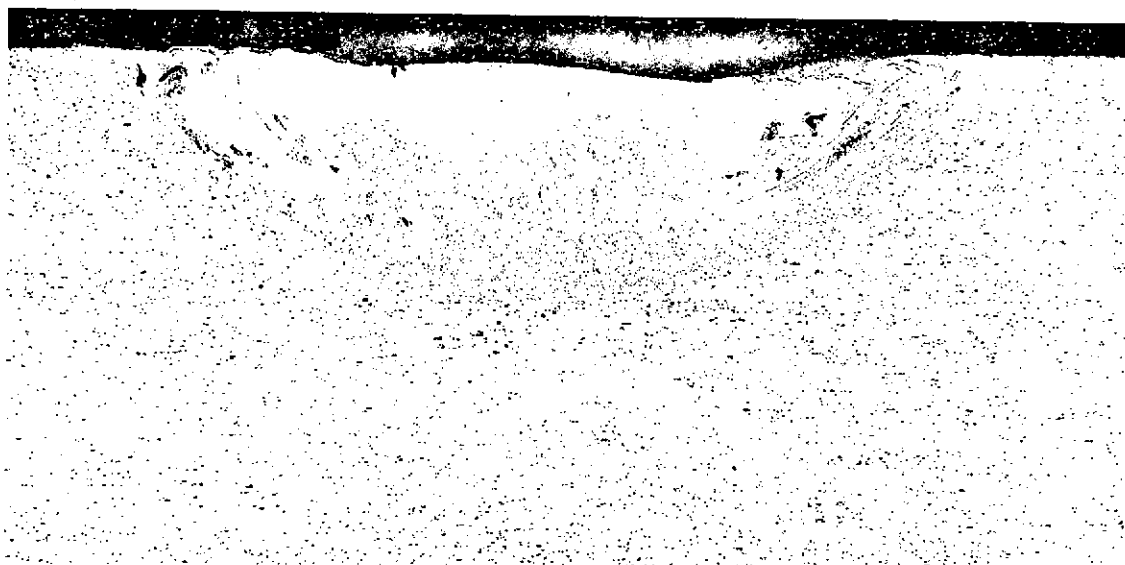


225°(-)

Etched

5G261-20X

FIGURE A-14. SECTION THROUGH FULL PENETRATION REGION- H-1

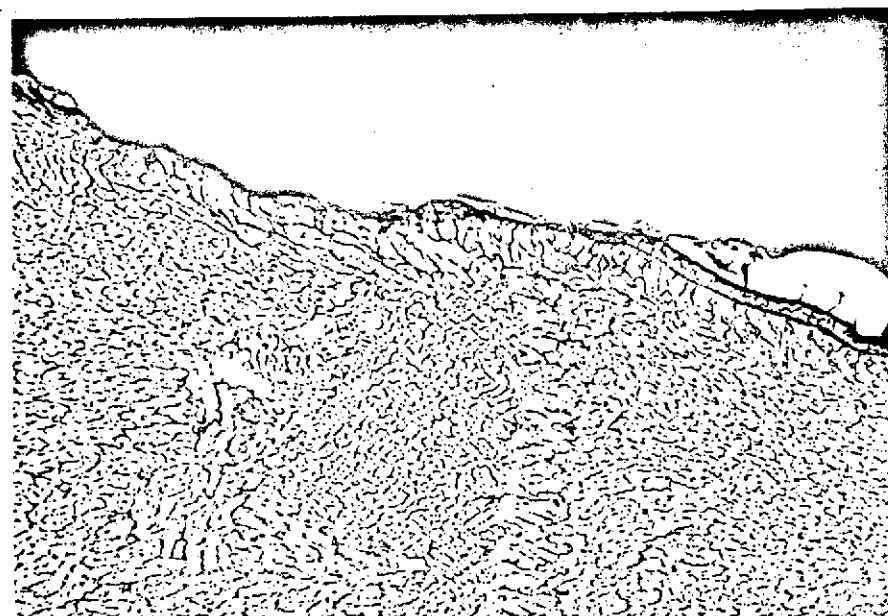


240°(+)

Etched

5G259-20X

FIGURE A-15. SECTION THROUGH PARTIAL PENETRATION REGION- H-1

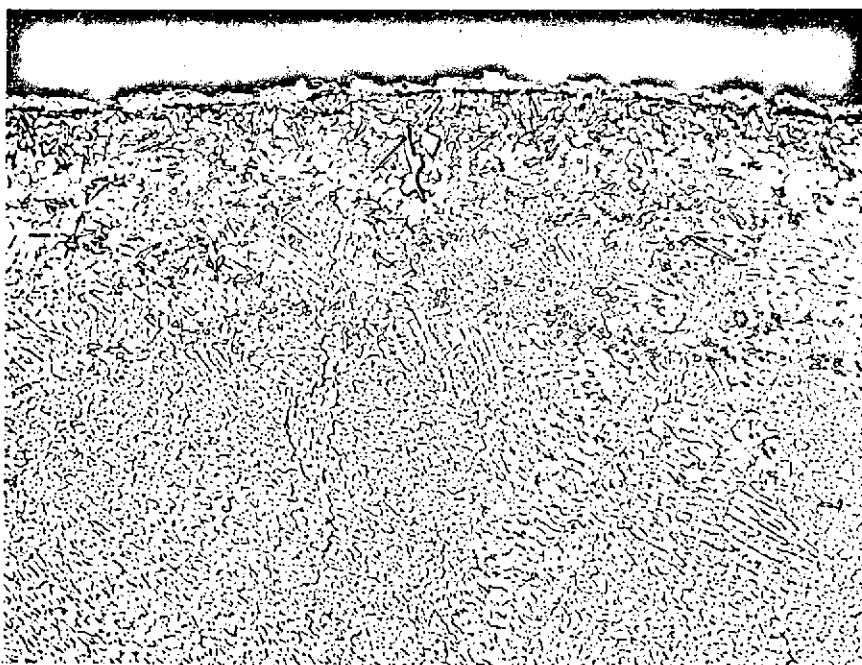


240°(+)

Etched

5G248-250X

FIGURE A-16. SECTION THROUGH UPPER LEFT
SURFACE OF PARTIAL PENETRATION
WELD- H-1



240°(+)

Etched

5G249-250X

FIGURE A-17. SECTION NEAR TOP SURFACE
PARTIAL PENETRATION WELD-
H-1

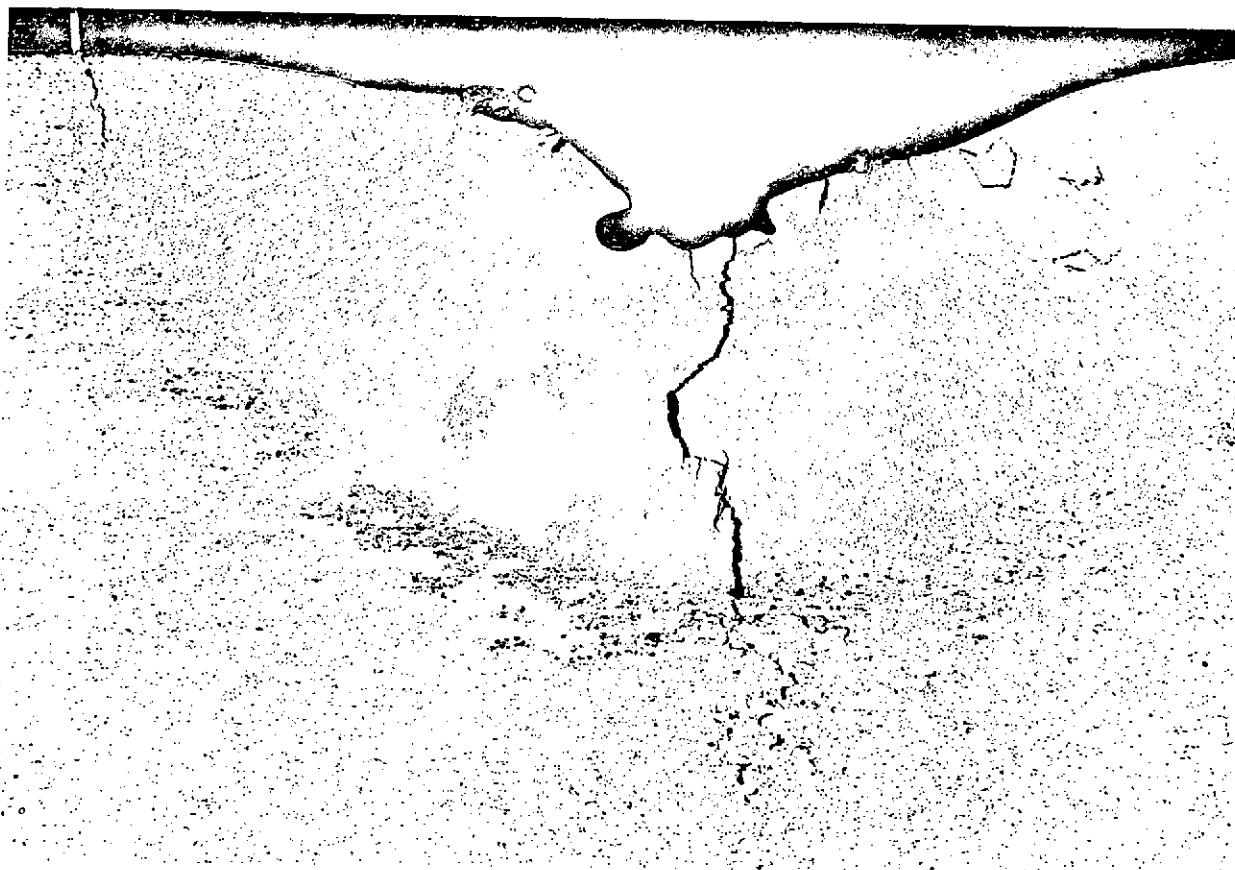


270°(-)

Etched

5G260-20X

FIGURE A-18. SECTION THROUGH PARTIAL PENETRATION REGION-
H-1

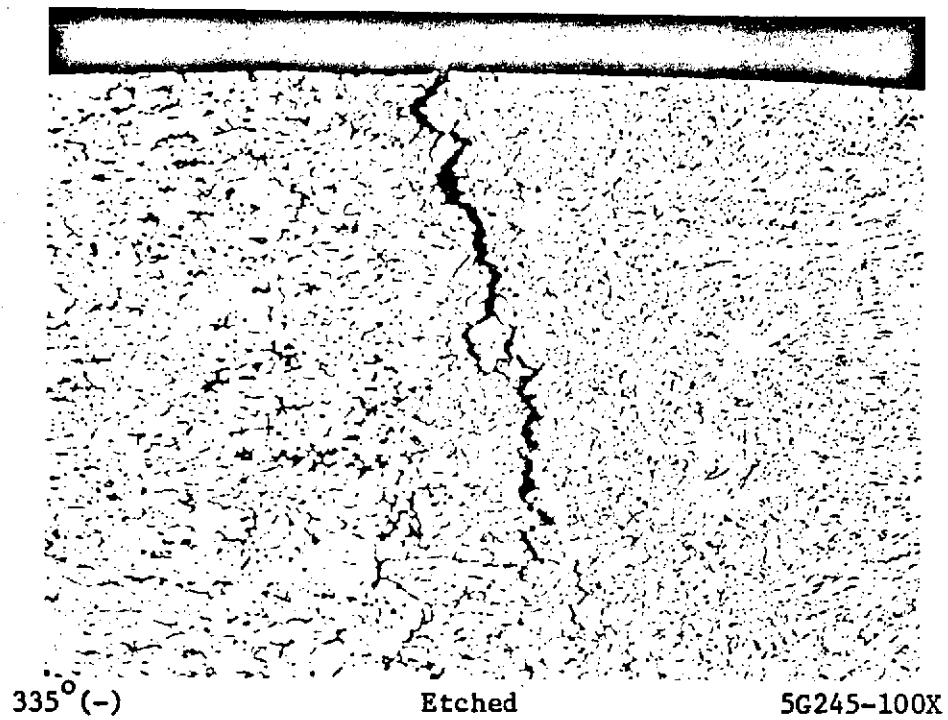


335°(-)

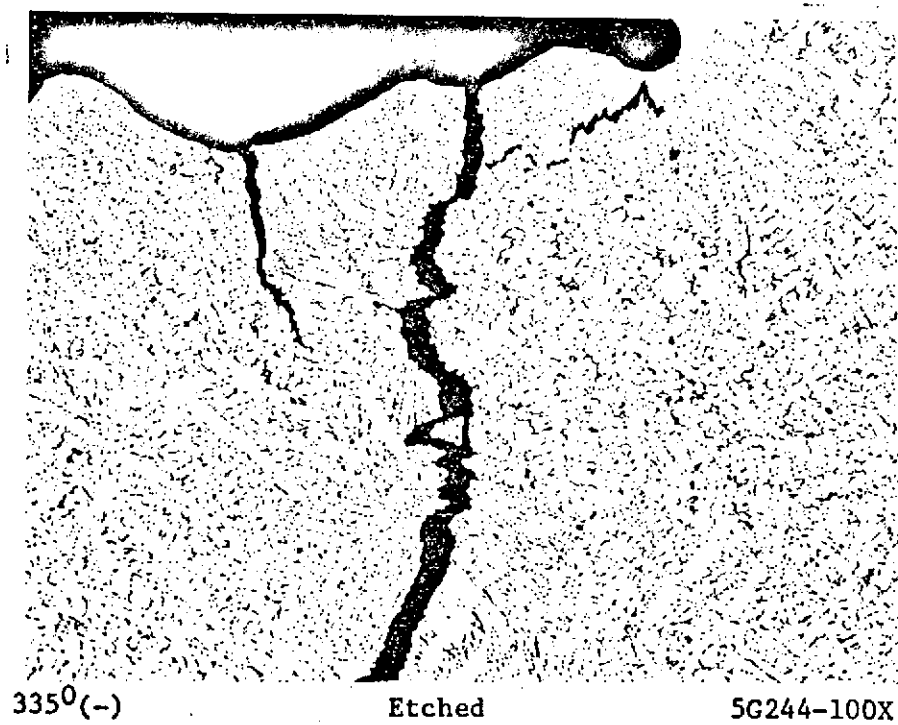
Etched

5G258-20X

FIGURE A-19. SECTION THROUGH DWELL REGION - H-1

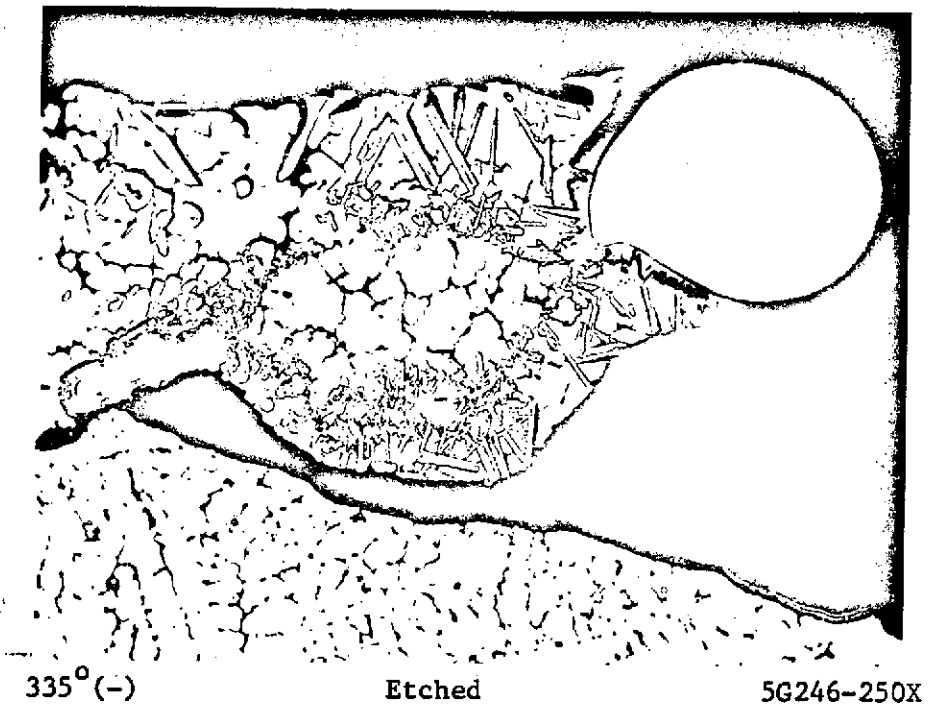


a. Crack near left edge in Figure A-19

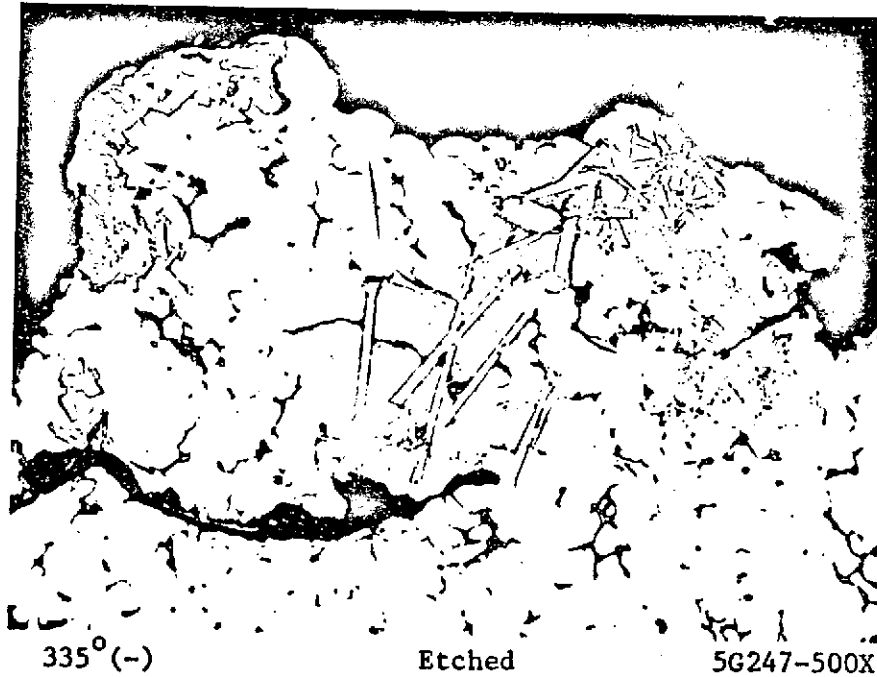


b. Main crack near center in Figure A-19

FIGURE A-20. CRACKS IN DWELL REGION- H-1



a. Near Left center in Figure A-19



b. Near right center in Figure A-19

FIGURE A-21. MOLYBDENUM TRACES ON SURFACES OF
DWELL REGION- H-1

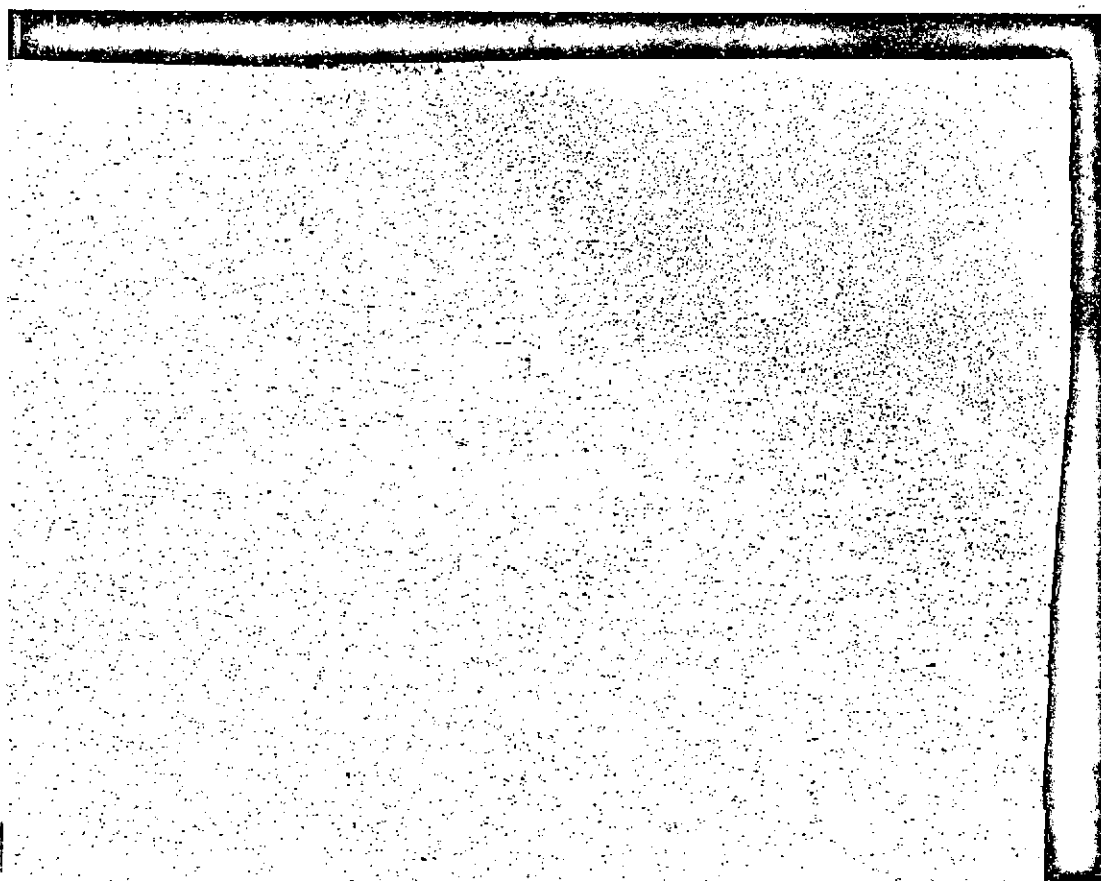


335°(-)

Etched

5G243-100X

FIGURE A-22. CRACKS NEAR TOP OF DWELL REGION- H-1



340°-335°

Etched

5G257-20X

FIGURE A-23. CHORD SECTION IN DWELL REGION- H-1



335°(-)

Aluminum

11299-300X

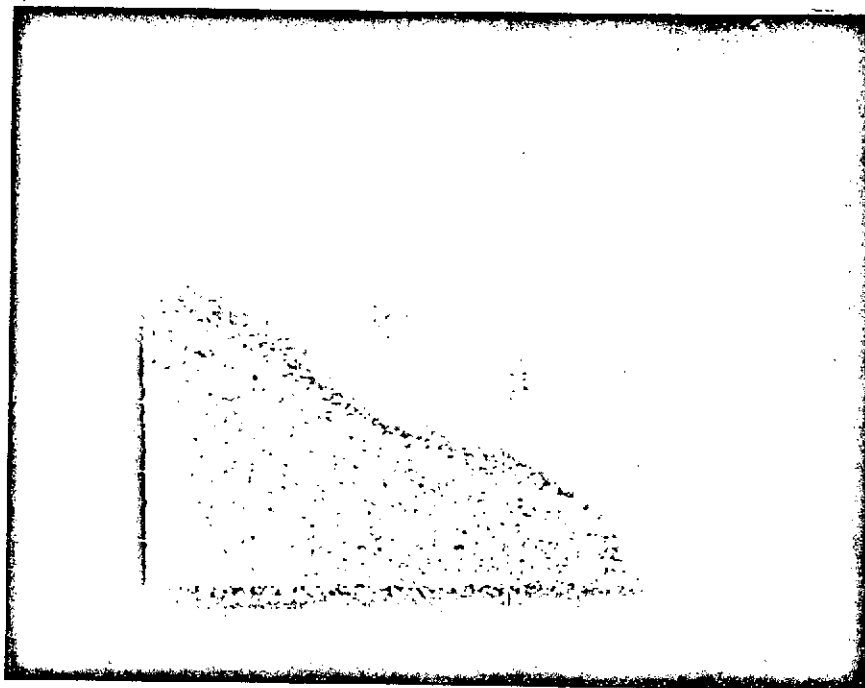


335°(-)

Molybdenum

11300-300X

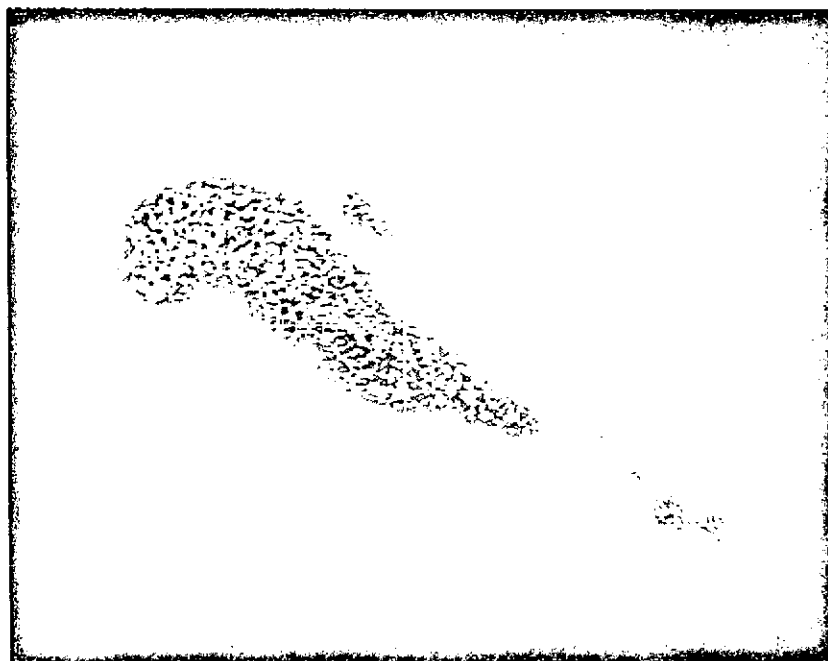
FIGURE A-24. ELECTRON PROBE SCANS OF REGION SHOWN IN FIGURE A-21 - LARGE PARTICLE AT LEFT CENTER ADJACENT TO END OF CREVICE - H-1



240°(+)

Aluminum

11301-300X

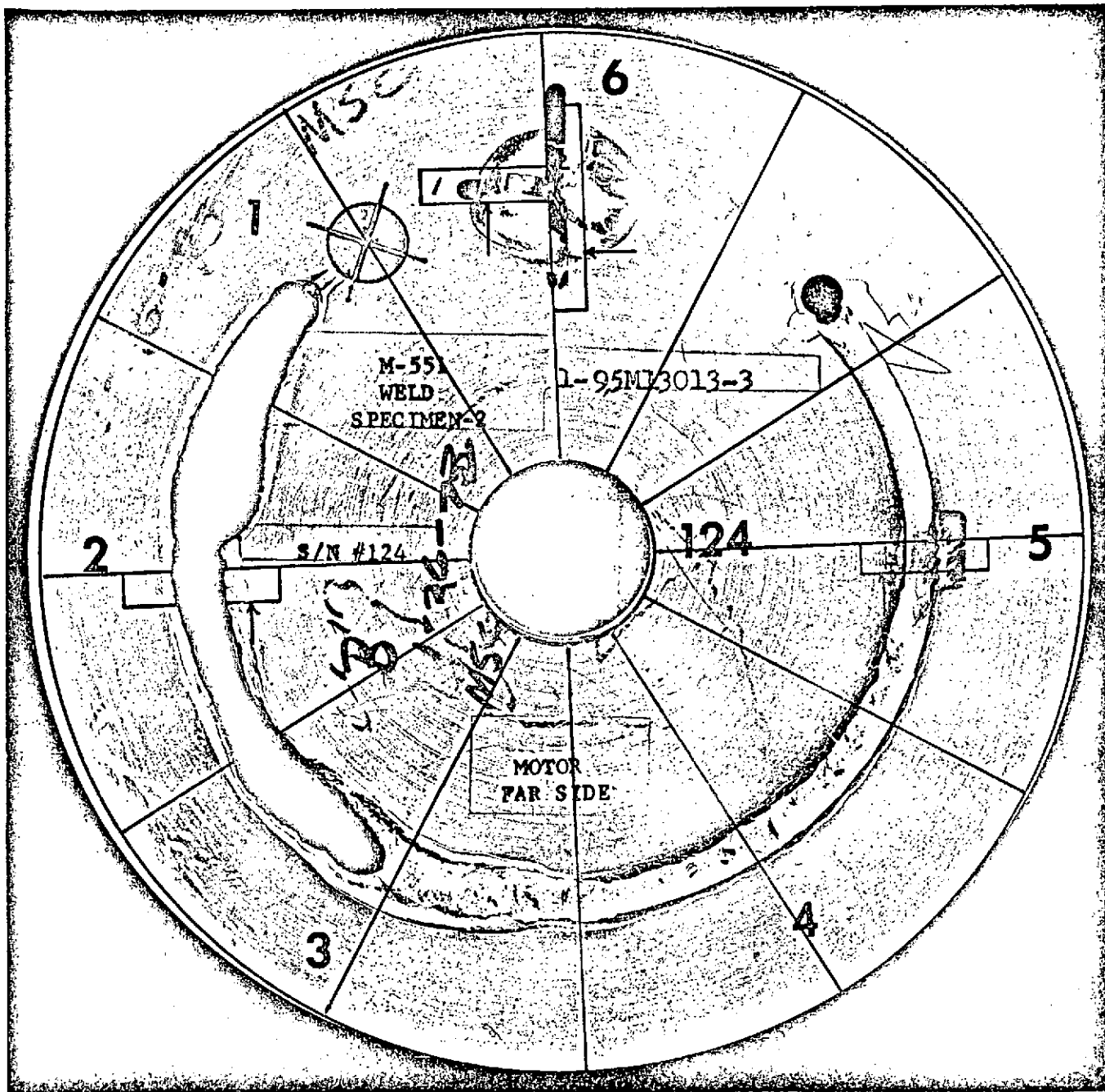


240°(+)

Molybdenum

11302-300X

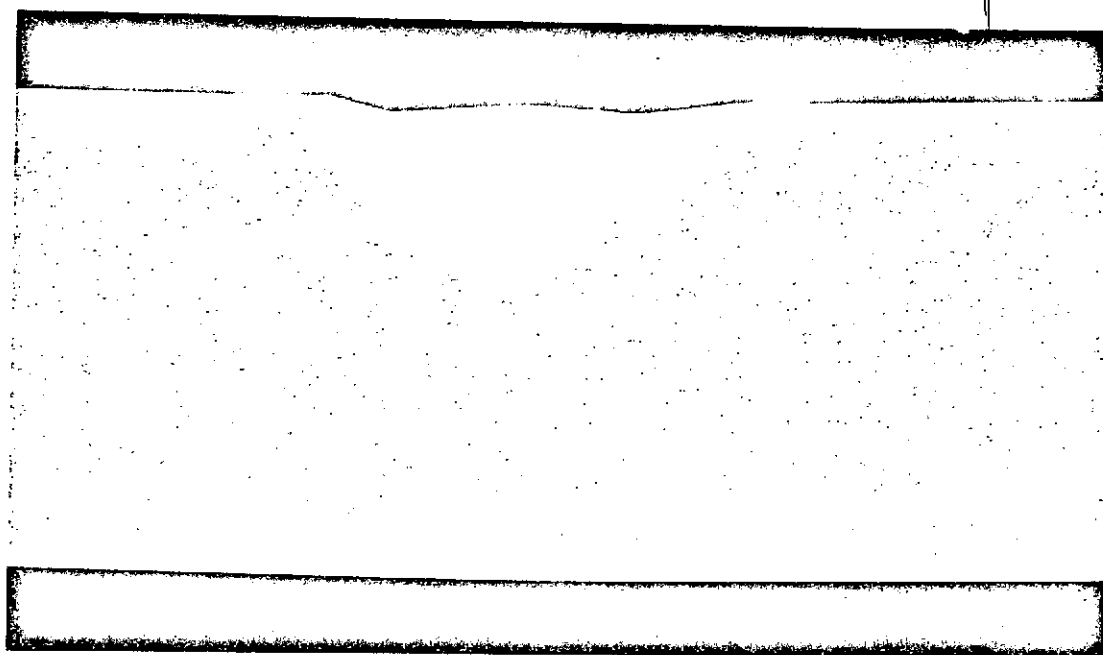
FIGURE A-25. ELECTRON PROBE SCANS OF REGION
SHOWN IN FIGURE A-16 - LARGE
PARTICLE AT TOP RIGHT SURFACE -H-1



Aluminum

5G443-1X

FIGURE A-26. FRONT SURFACE - S/N 124



240°(-)

Etched

7G483-10X

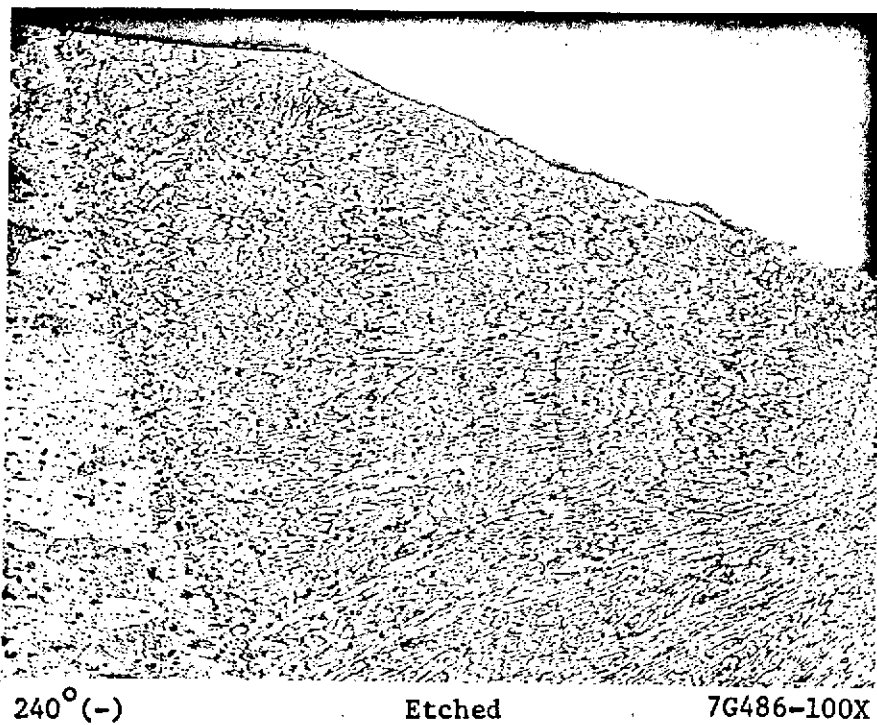


240°(-)

Etched

7G485-20X

FIGURE A-27. SECTION THROUGH PARTIAL PENETRATION
REGION - S/N-124

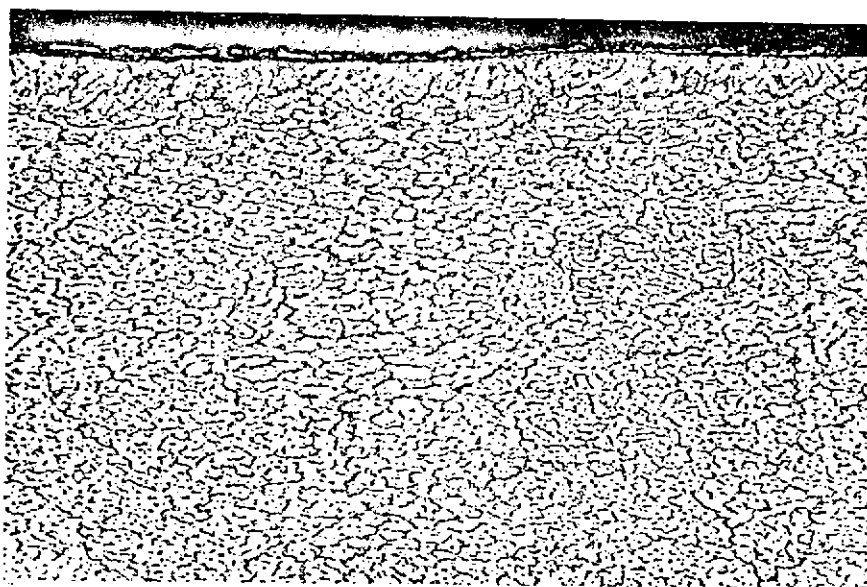


240°(-)

Etched

7G486-100X

a. Left fusion line



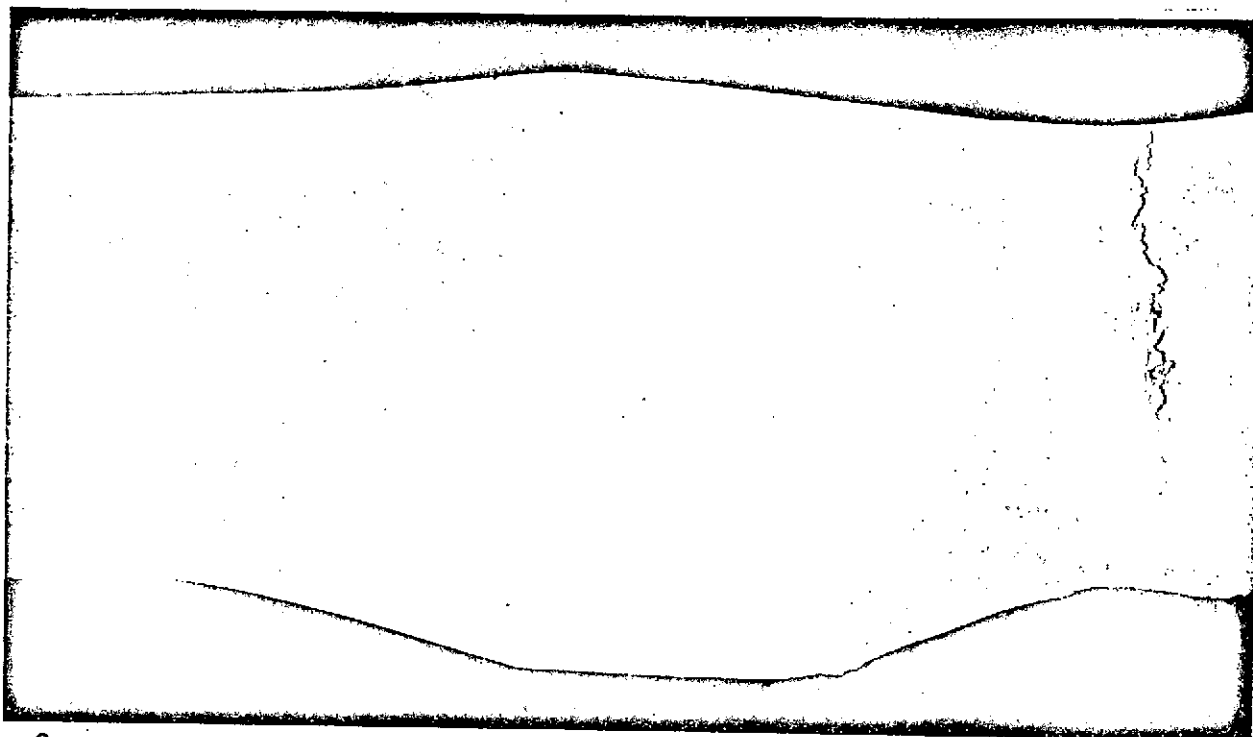
240°(-)

Etched

7G487-250X

b. Weld surface

FIGURE A-28. ENLARGED AREAS OF
STET PENETRATION REGION
S/N-124

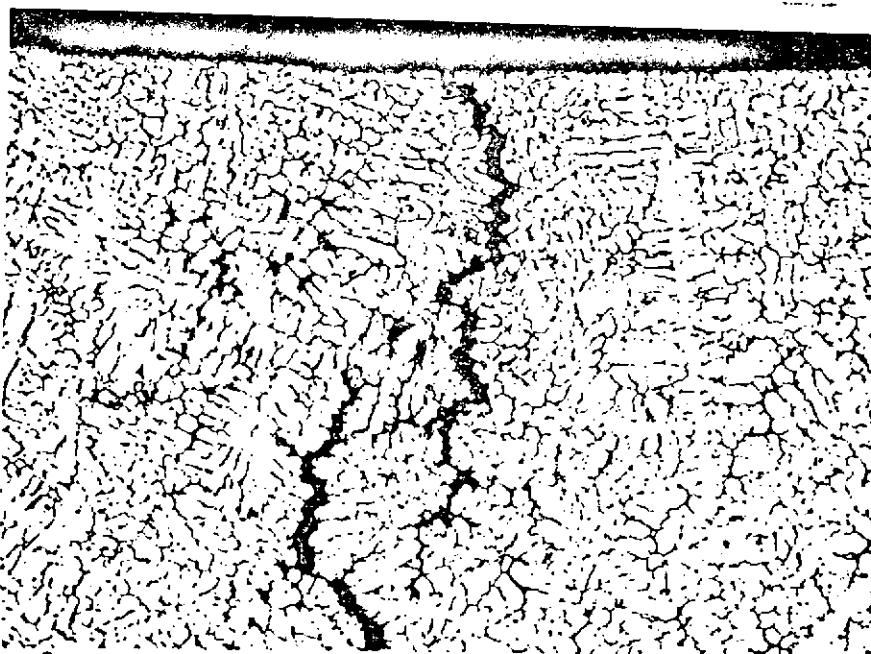


290° (+)

Etched

7G481-10X

FIGURE A-29. SECTION THROUGH DWELL REGION
S/N-124

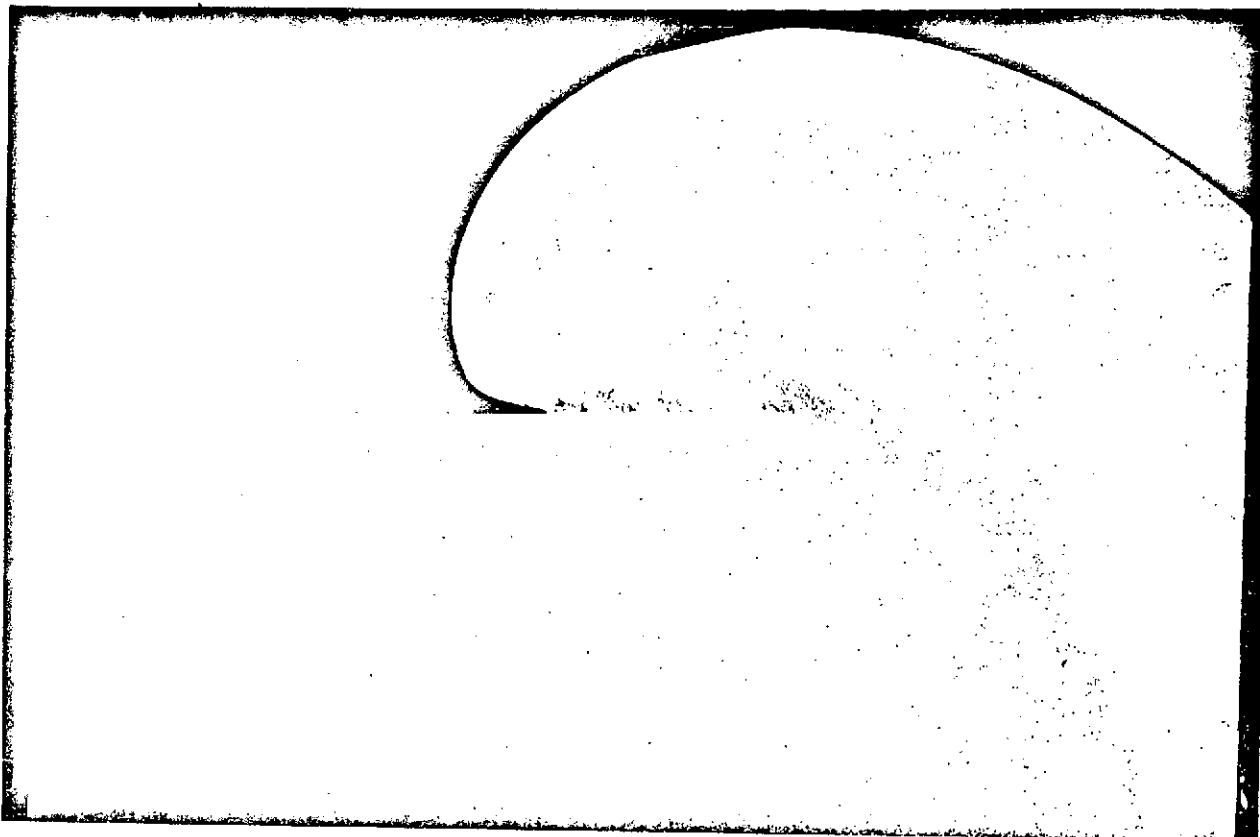


290° (+)

Etched

7G482-100X

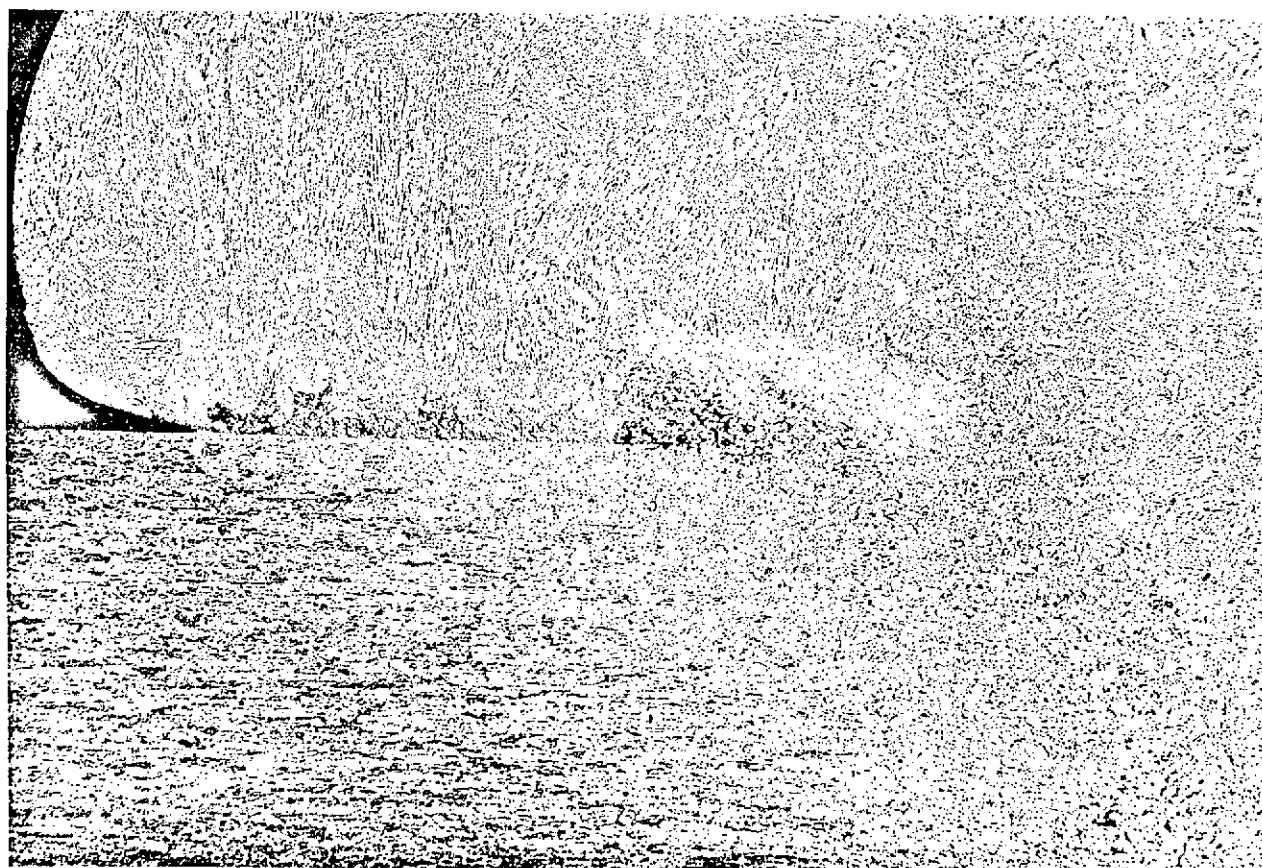
FIGURE A-30. SECTION THROUGH CRACK
IN DWELL REGION - S/N-124



350°-330°

Etched

7G476-10X



~ 340°

Etched

7G477-20X

FIGURE A-31. CHORD SECTION THROUGH DWELL REGION
S/N-124

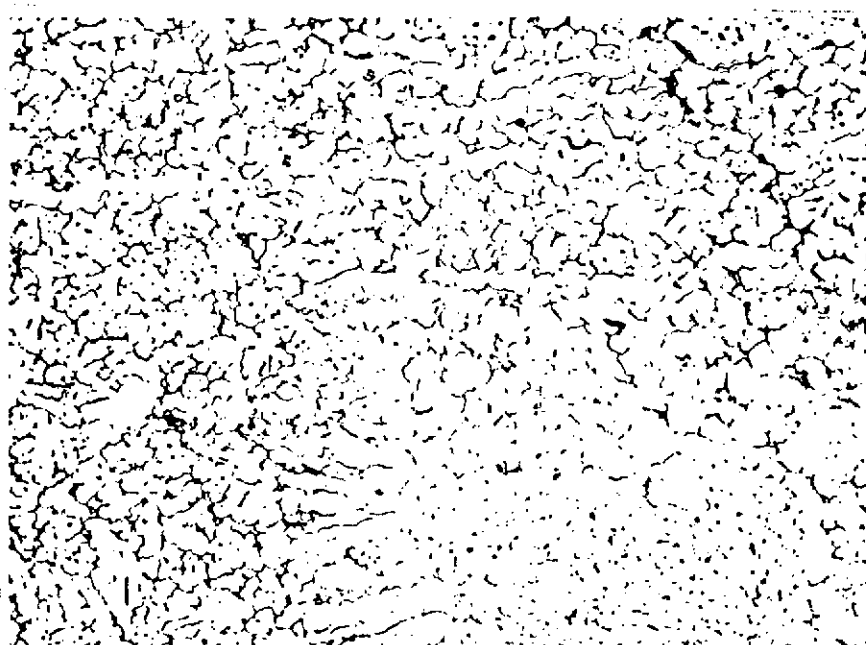


-340°

Etched

7G478-100X

a. Weld metal-base metal interface



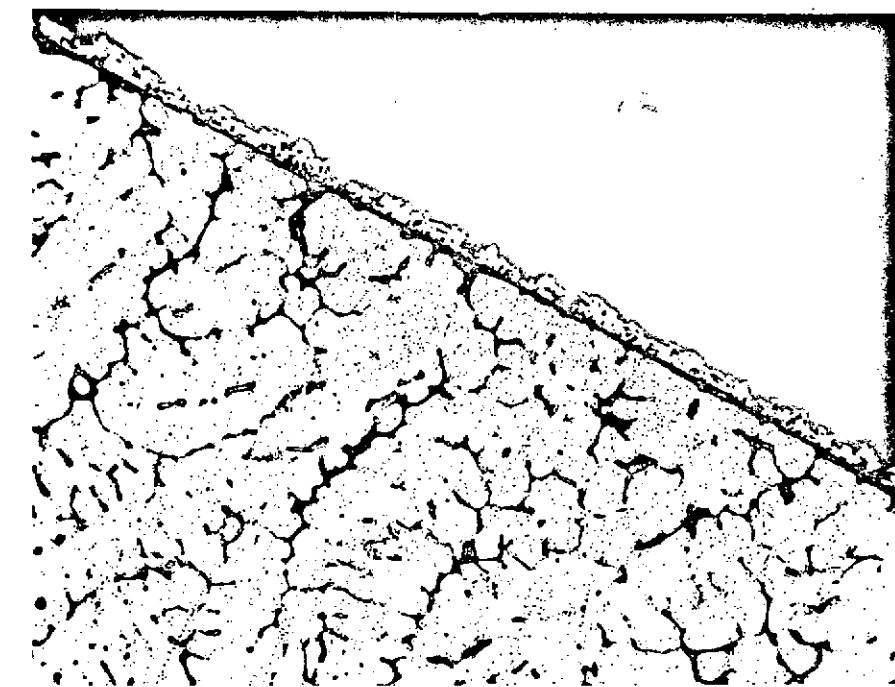
-335°

Etched

7G479-100X

b. Internal microstructure

FIGURE A-32. STRUCTURES IN DWELL REGION
S/N-124



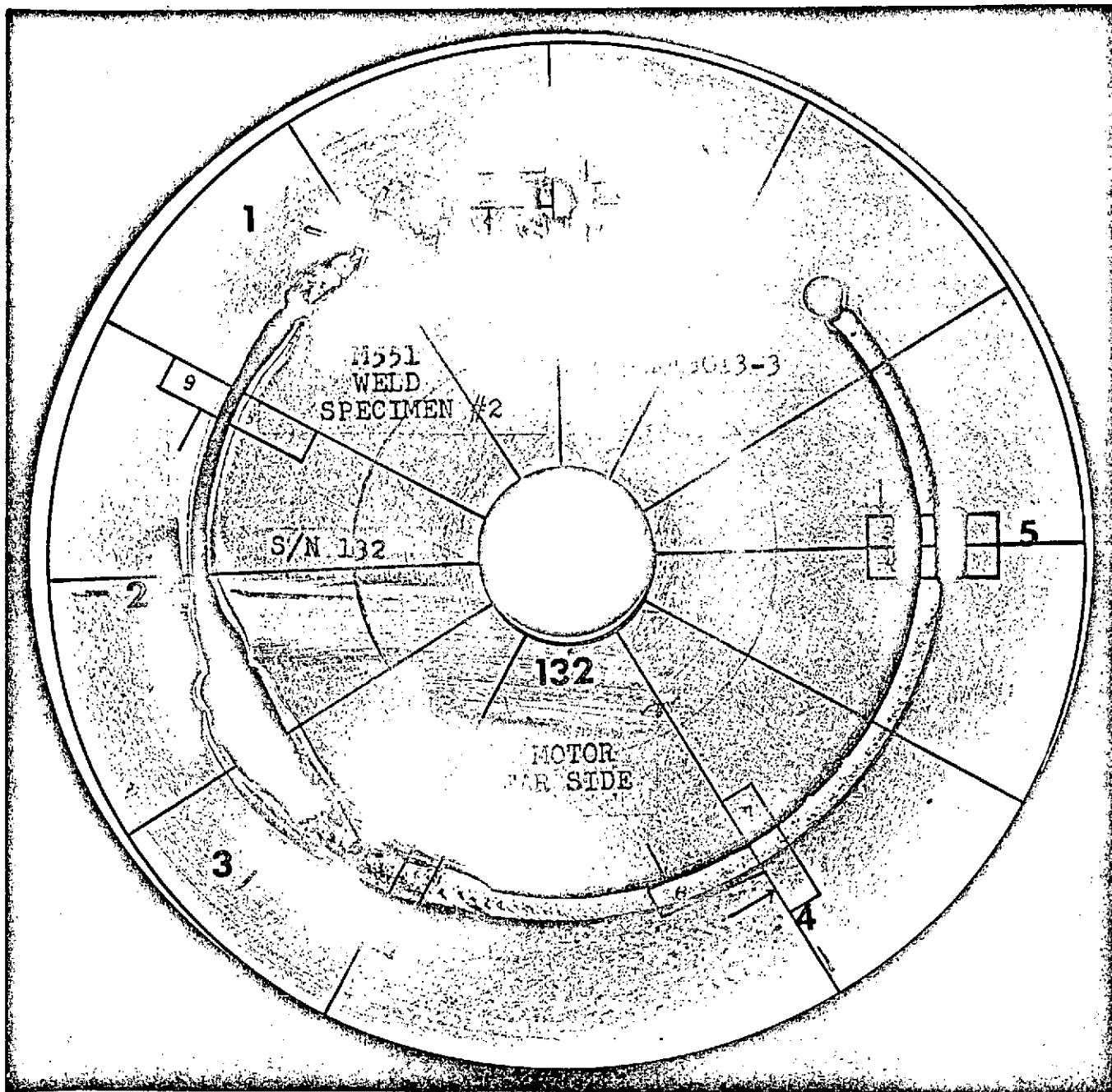
~330°

Etched

7G480-250X

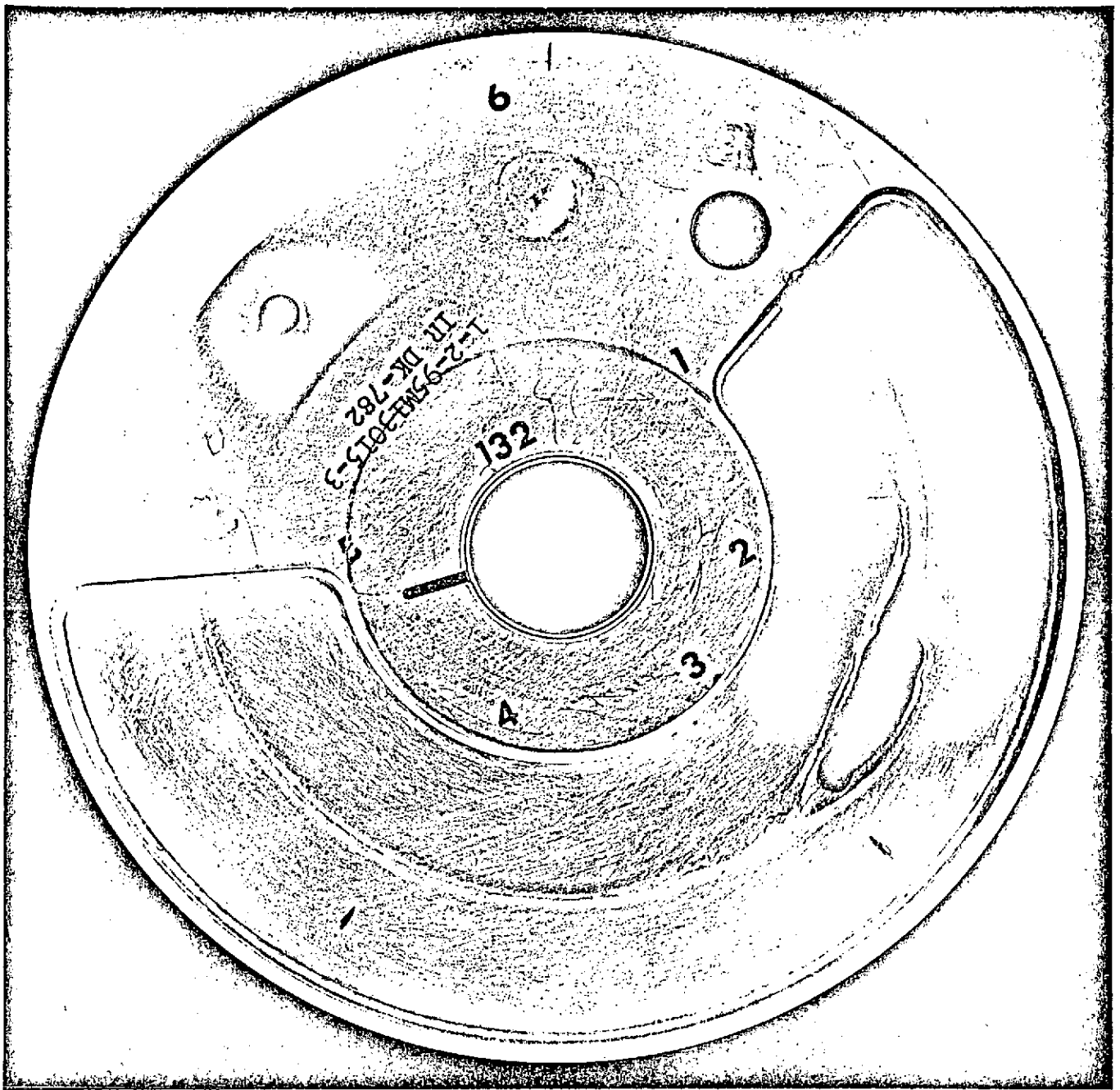
c. Surface microstructure

FIGURE A-32. (Continued)
STRUCTURES IN DWELL REGION
S/N-124



7G513-1X

FIGURE A-33. FRONT SURFACE -S/N 132



7G512-1X

FIGURE A-34. BACK SURFACE - S/N 133

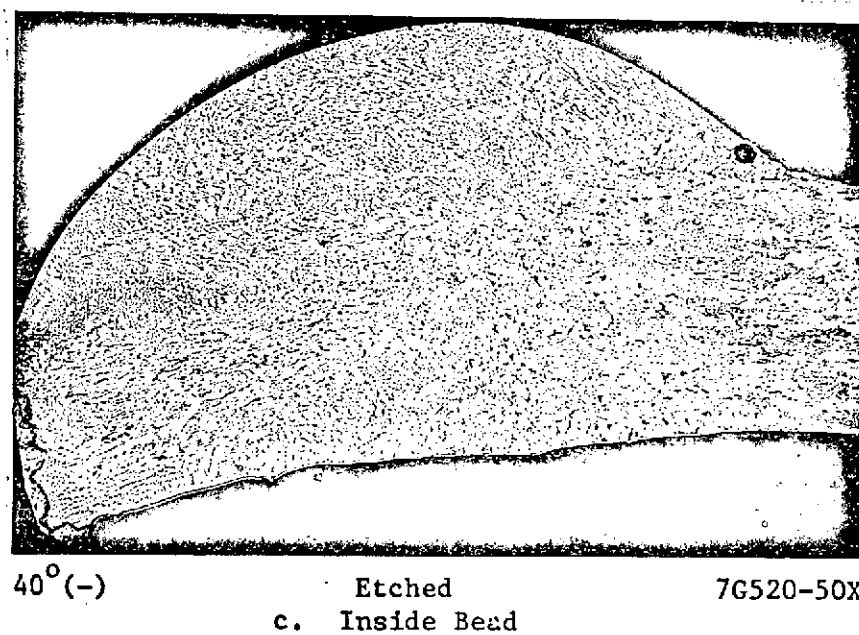
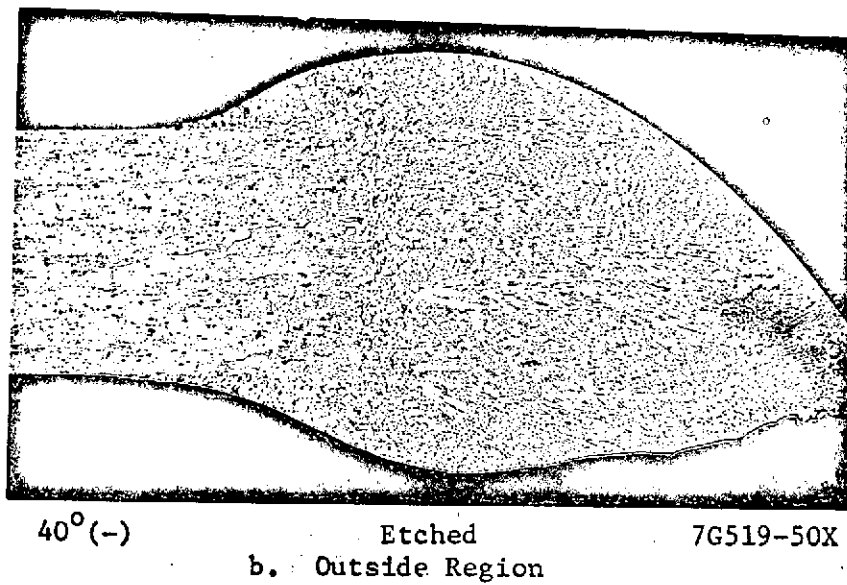
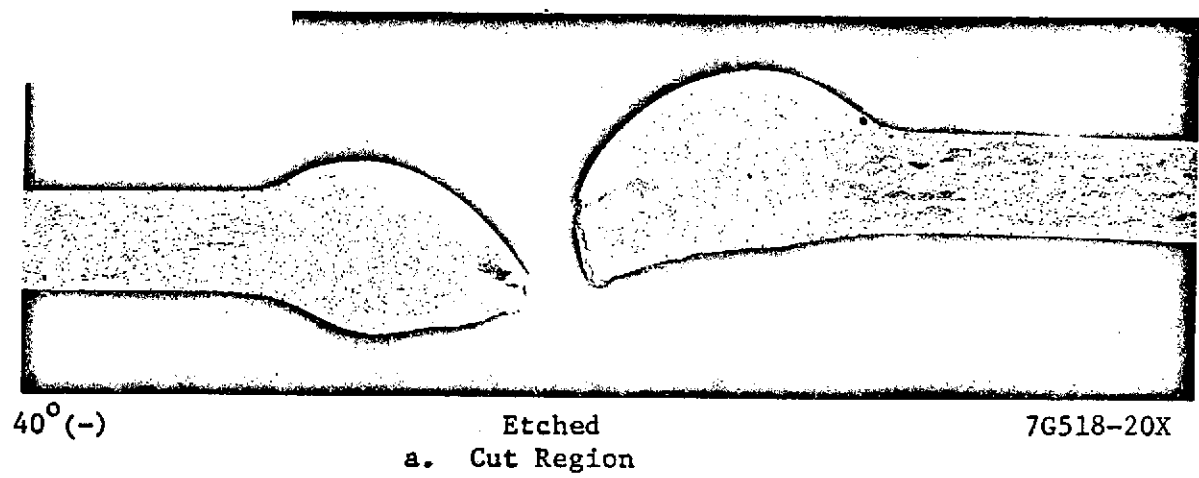


FIGURE A-35. SECTION THROUGH CUT
REGION - S/N 132

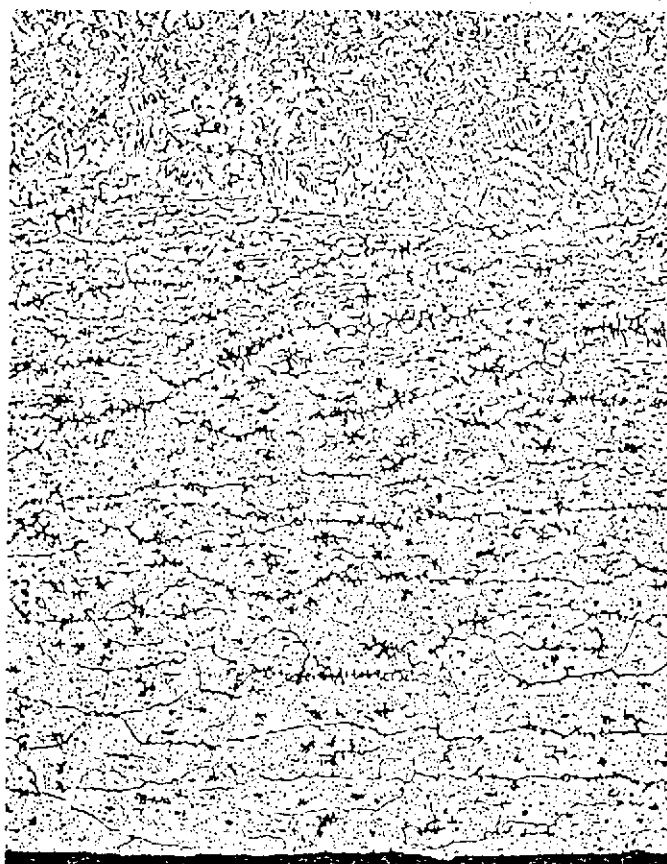


165°-180°

Etched

7G516-20X

a. Complete section



~170°

Etched

7G517-100X

b. Bottom fusion line

FIGURE A-36. CHORD SECTION IN FULL PENETRATION REGION S/N 132

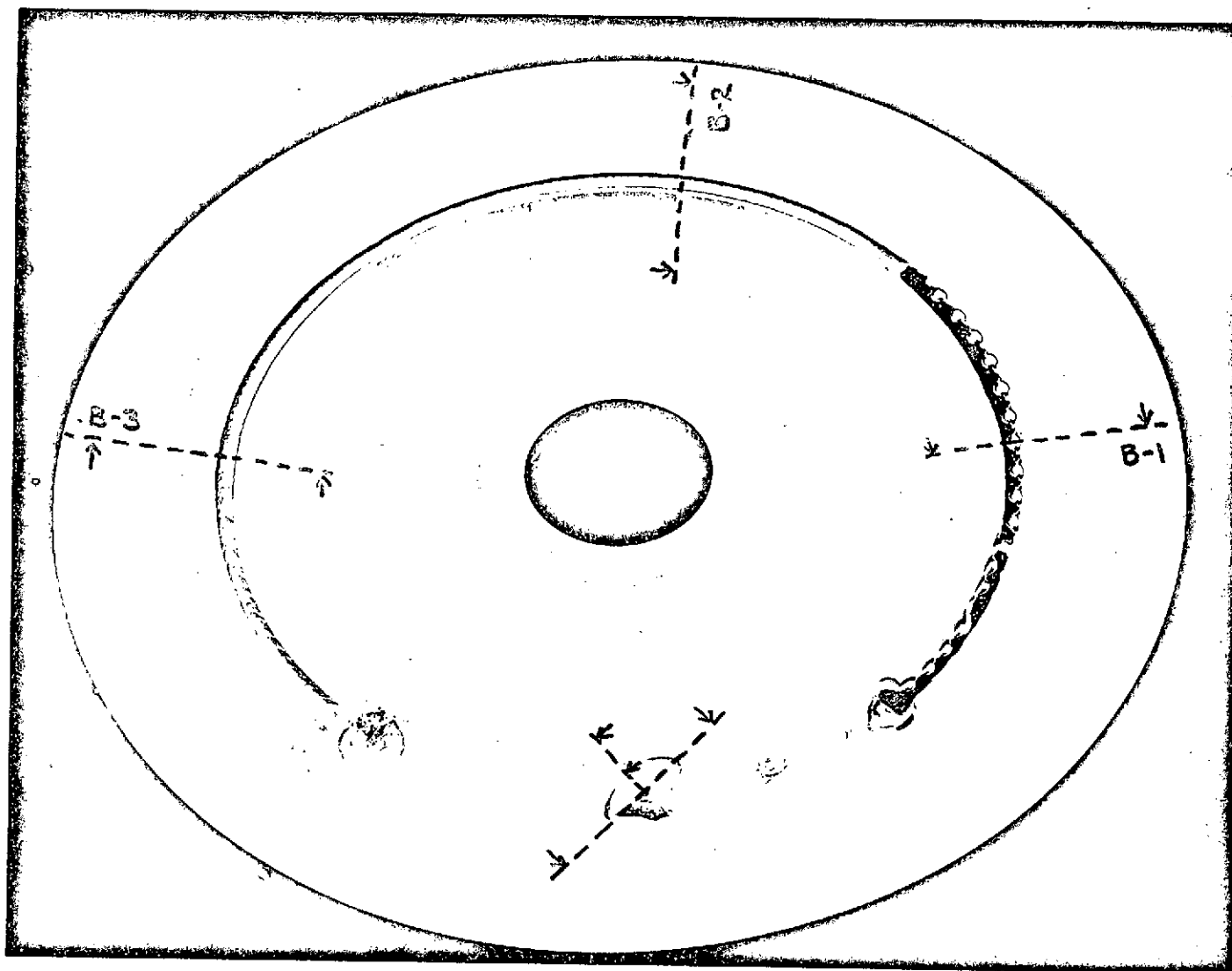
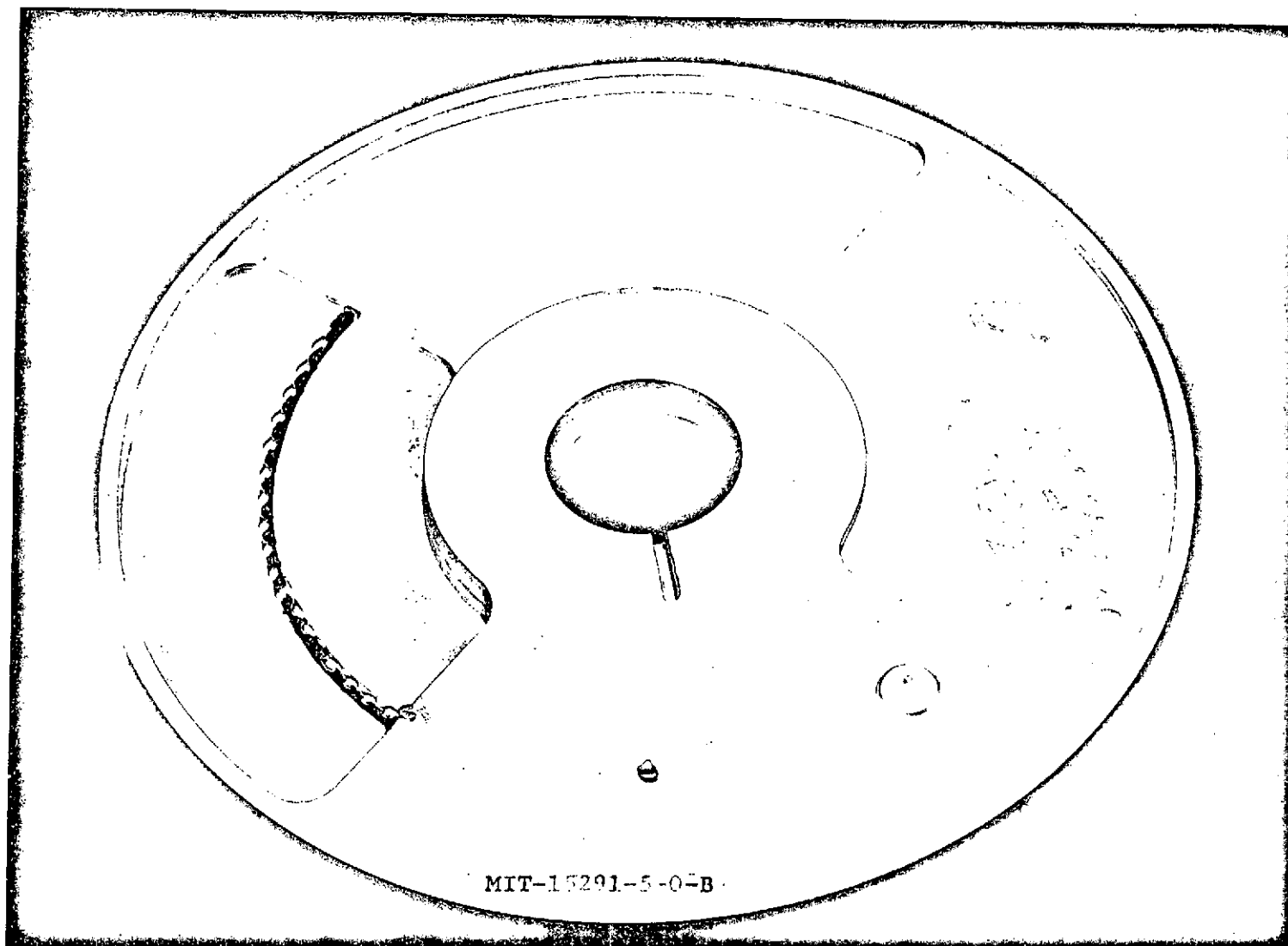


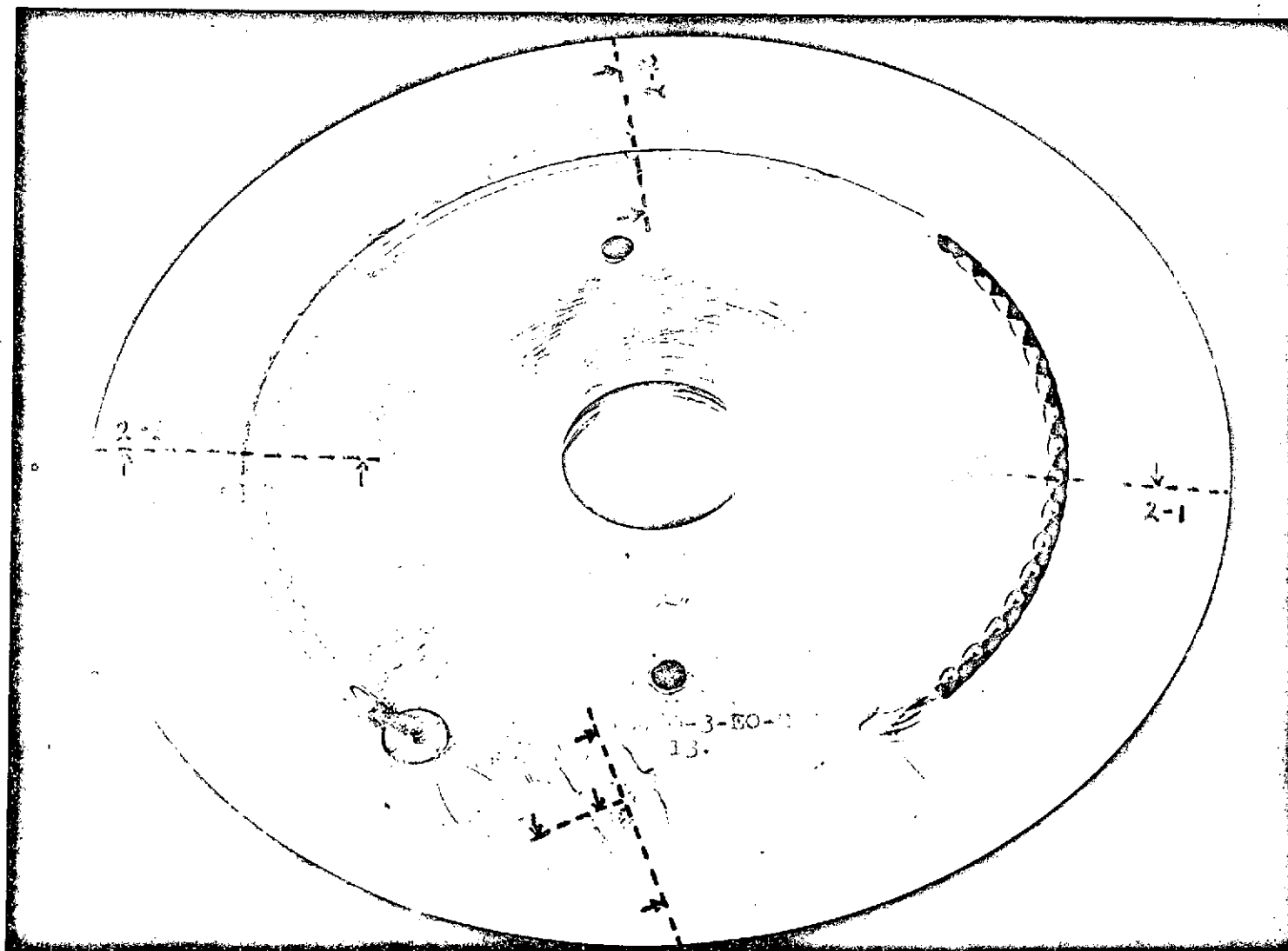
FIGURE A-37. FRONT OF DISC B SHOWING SECTION LOCATIONS

5112-~/X



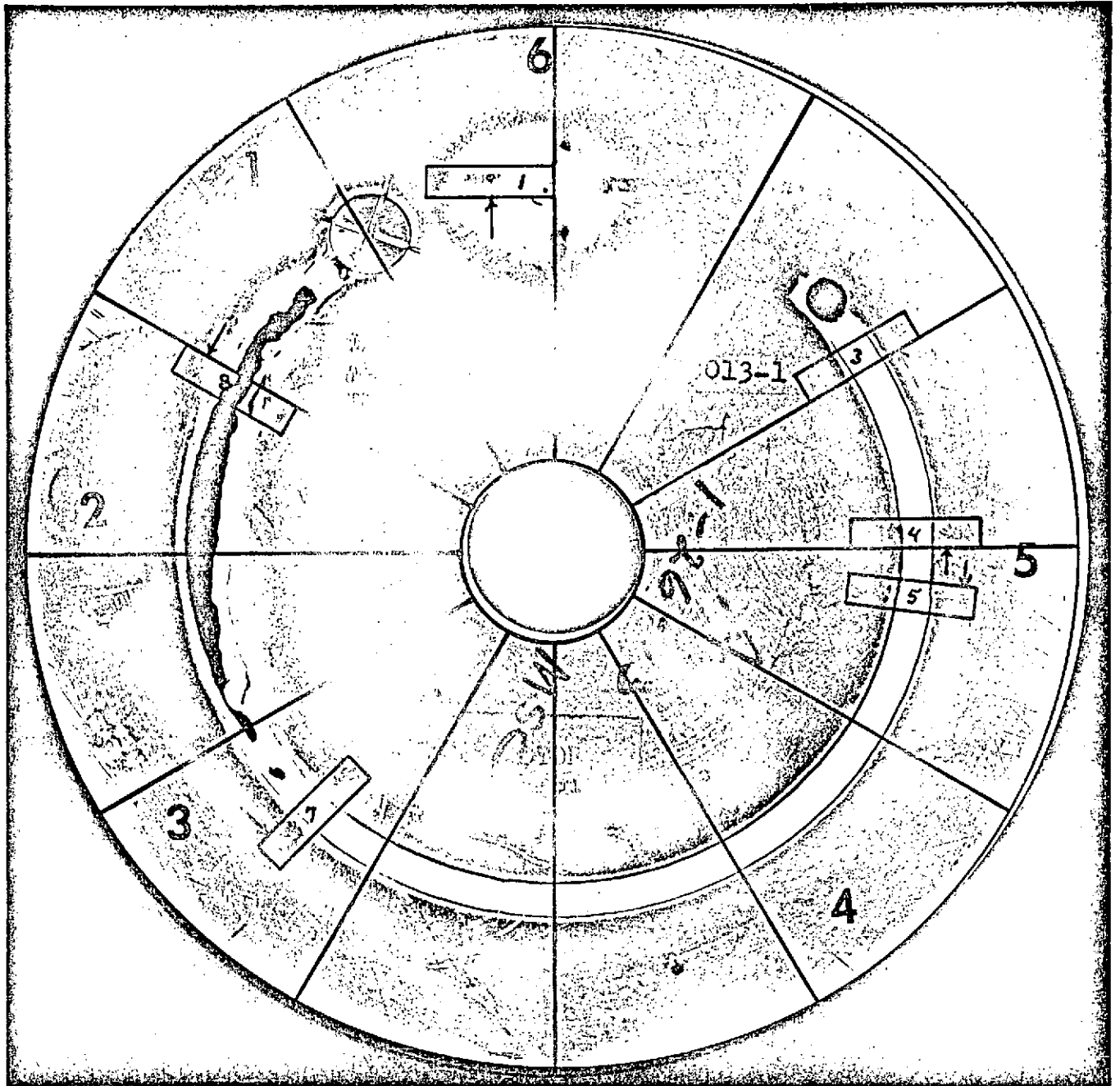
5111-~/X

FIGURE A-38. BACK OF DISC B SHOWING QUADRANT DESIGN



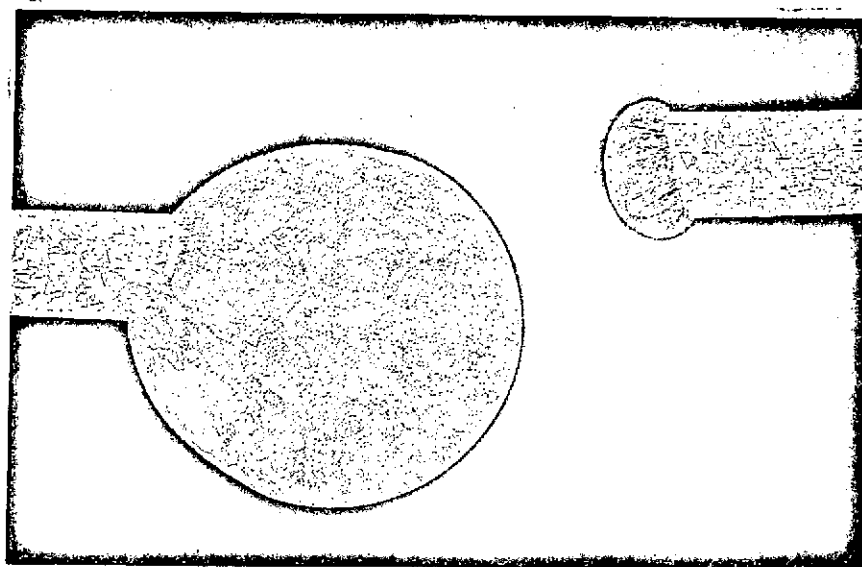
5113-~/X

FIGURE A-39. FRONT OF DISC 2 SHOWING SECTION LOCATIONS



5G442-1X

FIGURE A-40. FRONT SURFACE - S/N 104

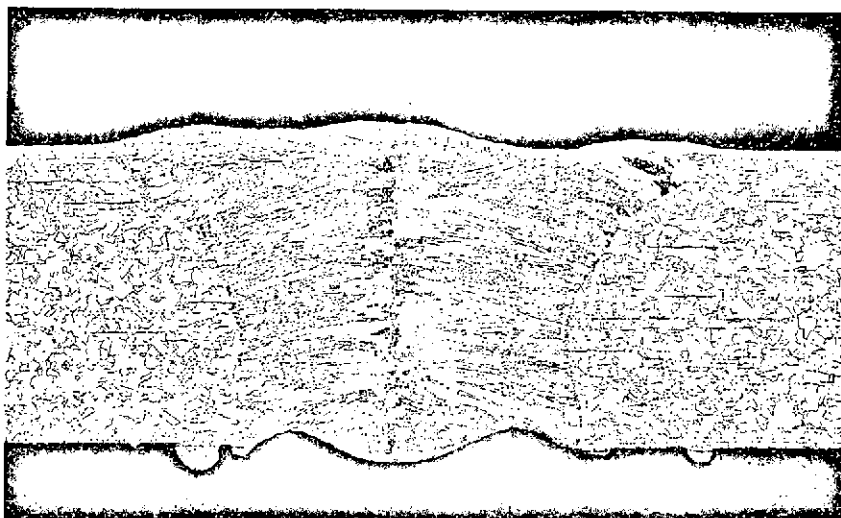


30°(+)

Etched

7G500-20X

FIGURE A-41. SECTION THROUGH CUT
REGION - S/N 104



105°(+)

Etched

7G498-20X

FIGURE A-42. SECTION THROUGH RAMP
REGION - S/N 104

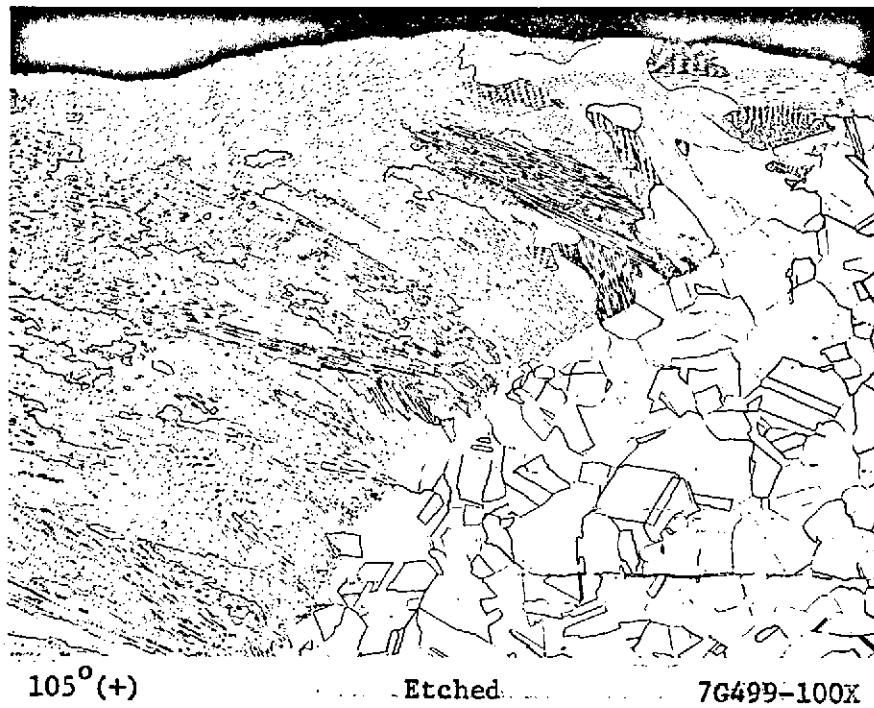


FIGURE A-43. FUSION LINE REGION
S/N 104

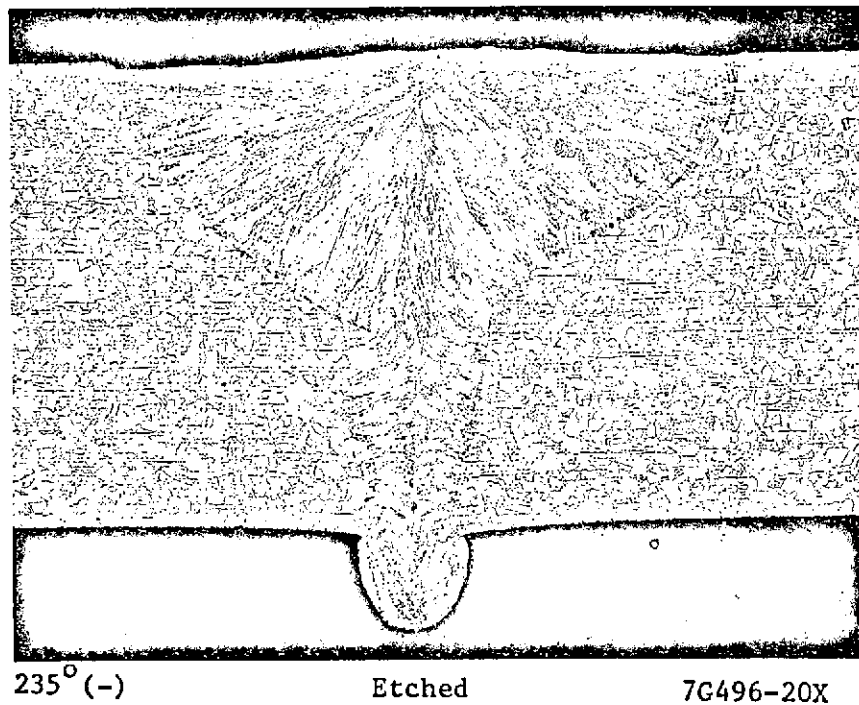


FIGURE A-44. SECTION THROUGH FULL
PENETRATION REGION
S/N 104

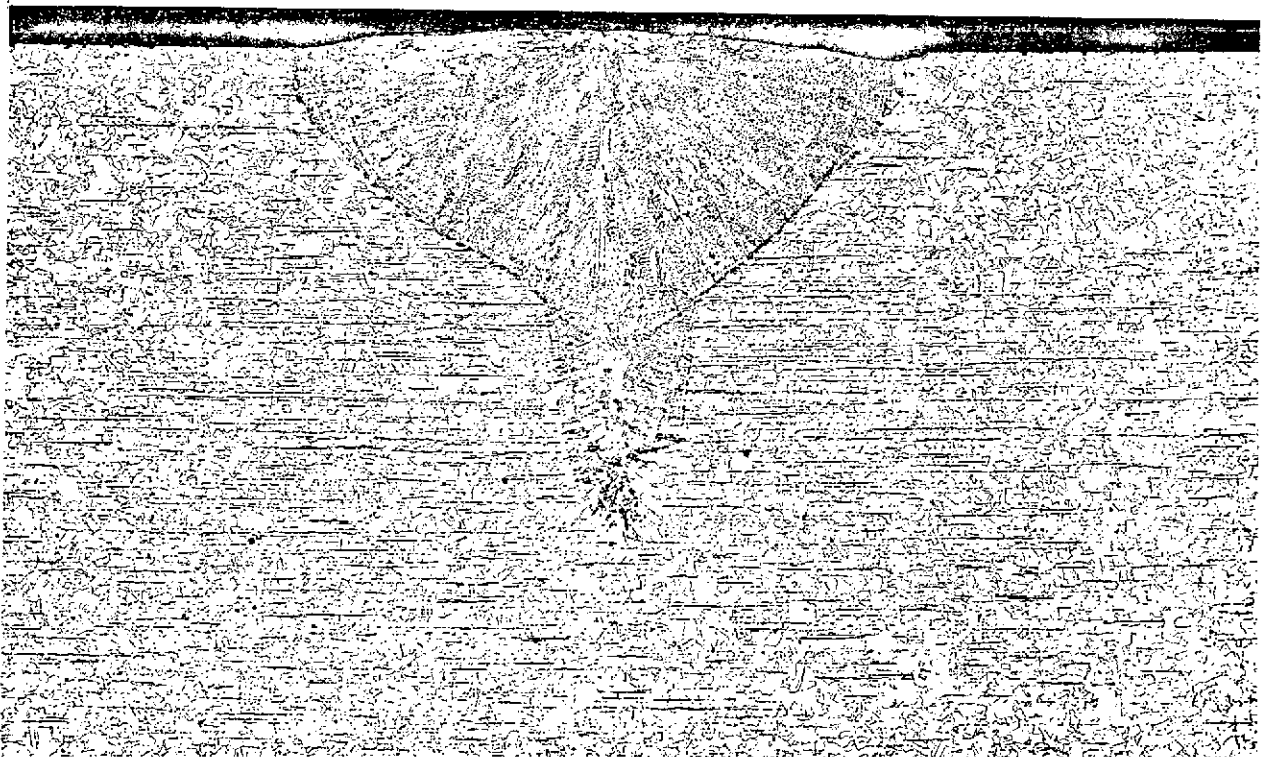


235°(-)

Etched

7G497-100X

FIGURE A-45. SECTION AT ROOT OF WELD S/N 104

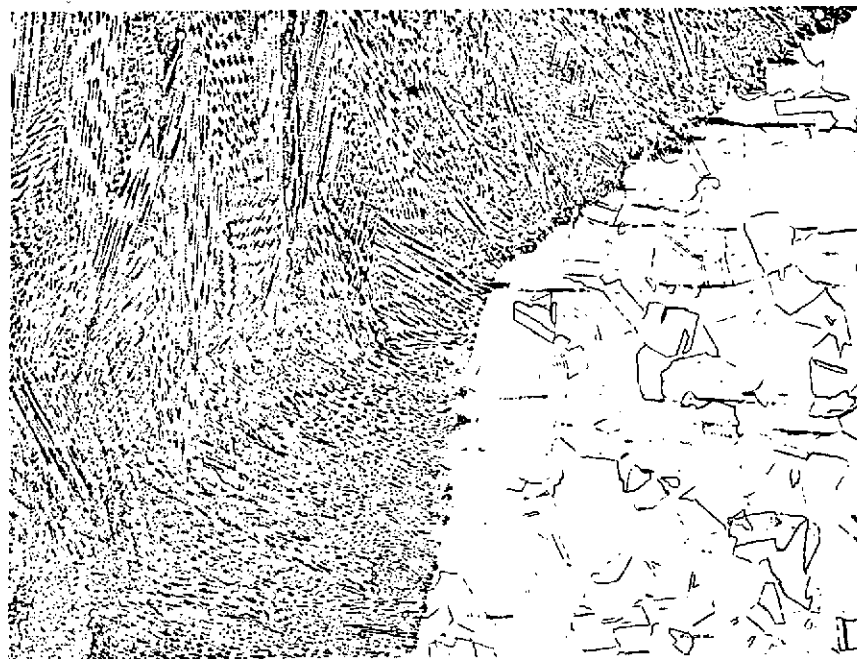


240°(+)

Etched

7G494-20X

FIGURE A-46. SECTION THROUGH PARTIAL PENETRATION
REGION - S/N 104



240°(+)

Etched

7G495-100X

FIGURE A-47. FUSION LINE REGION.
AT SHAPE CHANGE S/N 104

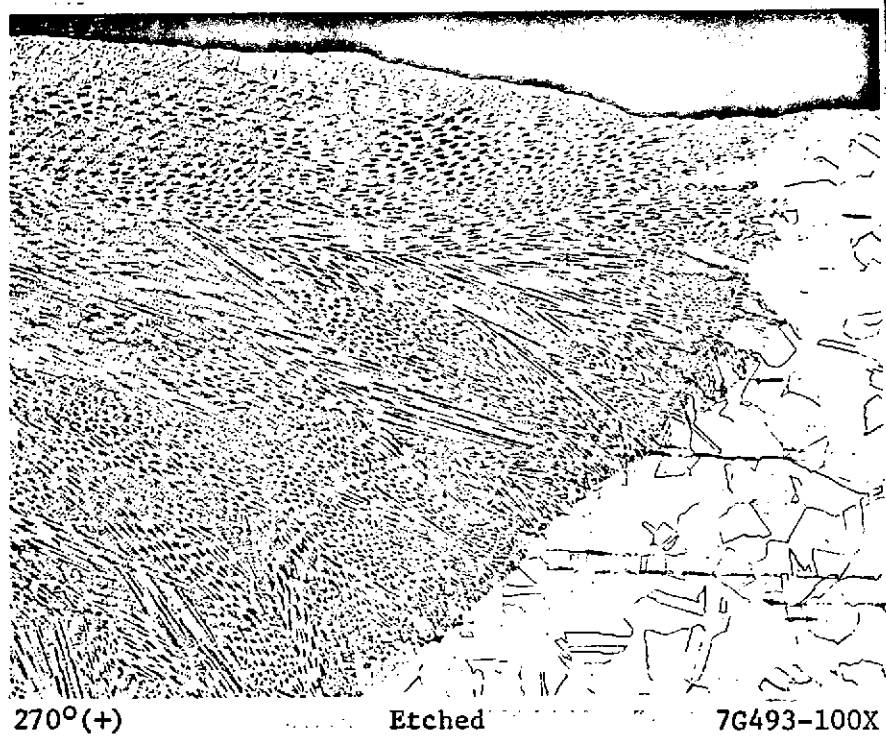


270°(+)

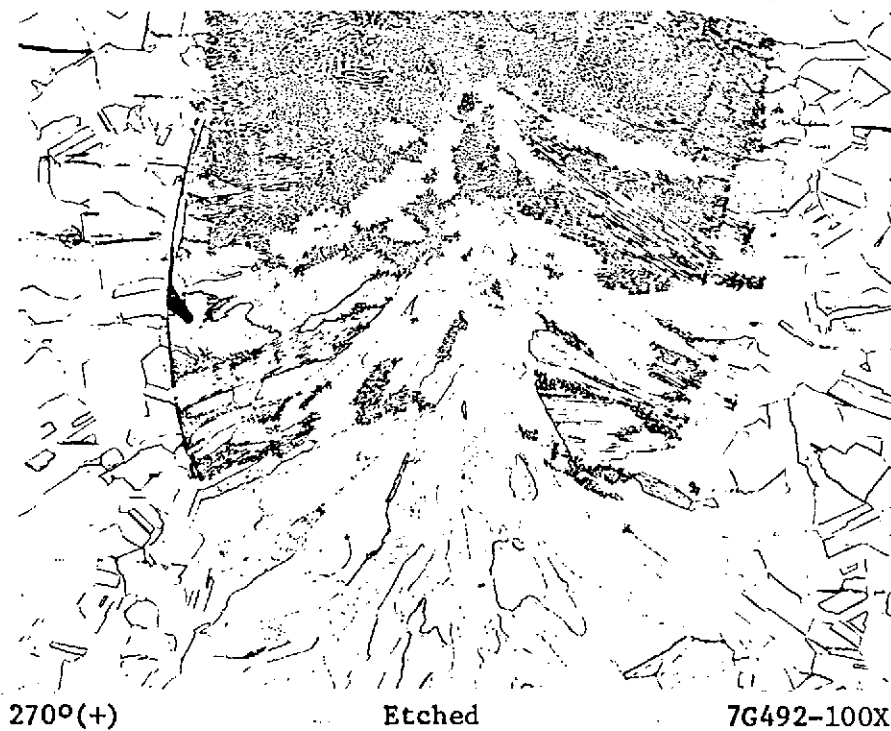
Etched

7G491-20X

FIGURE A-48. SECTION THROUGH PARTIAL PENETRATION
REGION S/N 104



a. Fusion Line at Top



b. Root of Weld

FIGURE A-49. WELD STRUCTURES - S/N 104



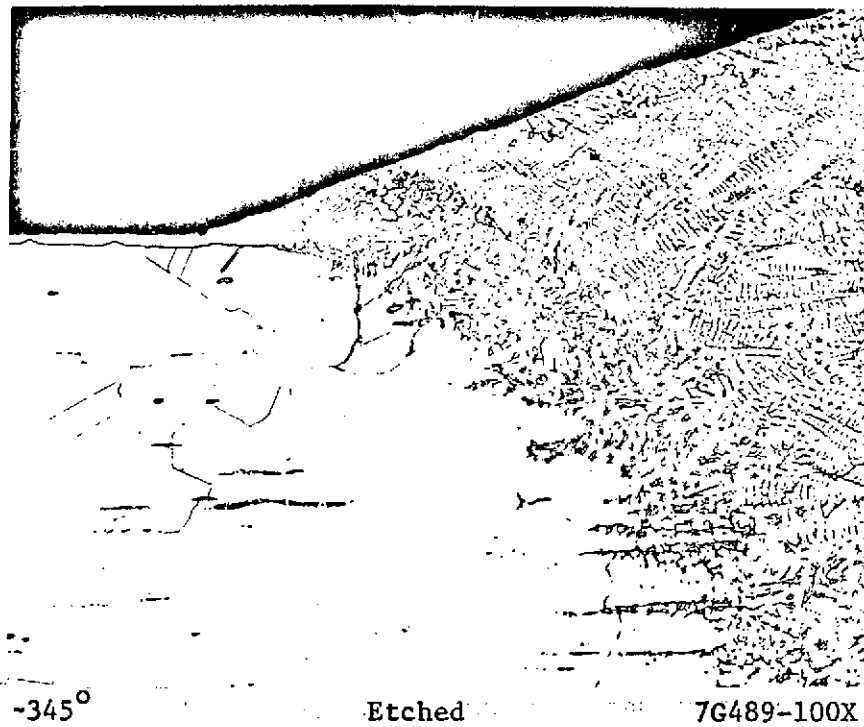
345°-330°

Etched

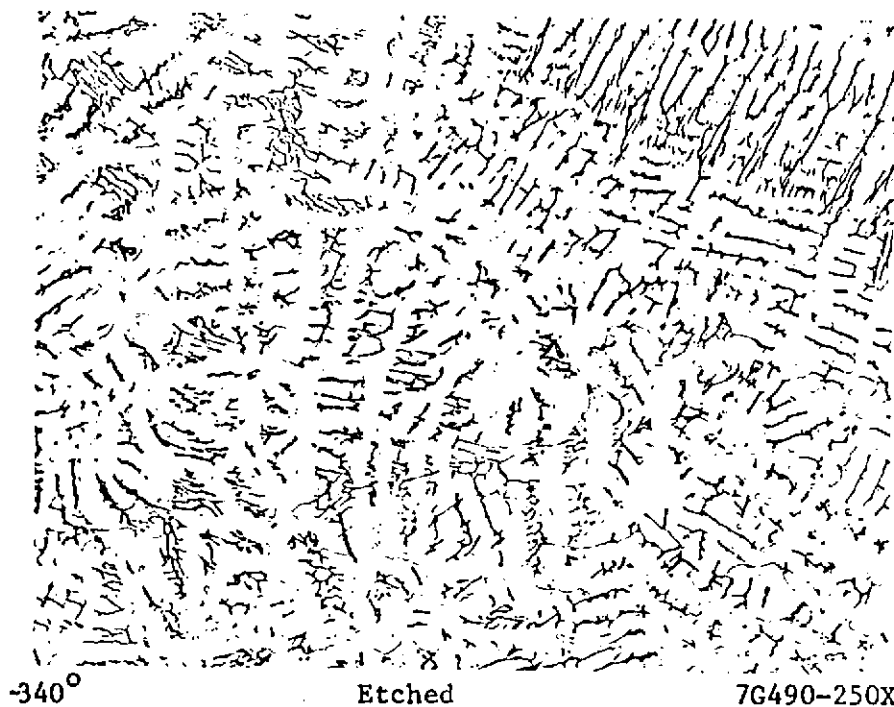
7G488-20X

a. Chord Section

FIGURE A-50. SECTIONS THROUGH DWELL REGION, S/N 104



b. Top Edge Fusion Line



c. Typical Weld Microstructure

FIGURE A-50. (Continued)
SECTIONS THROUGH DWELL REGION
S/N 104

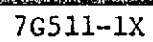
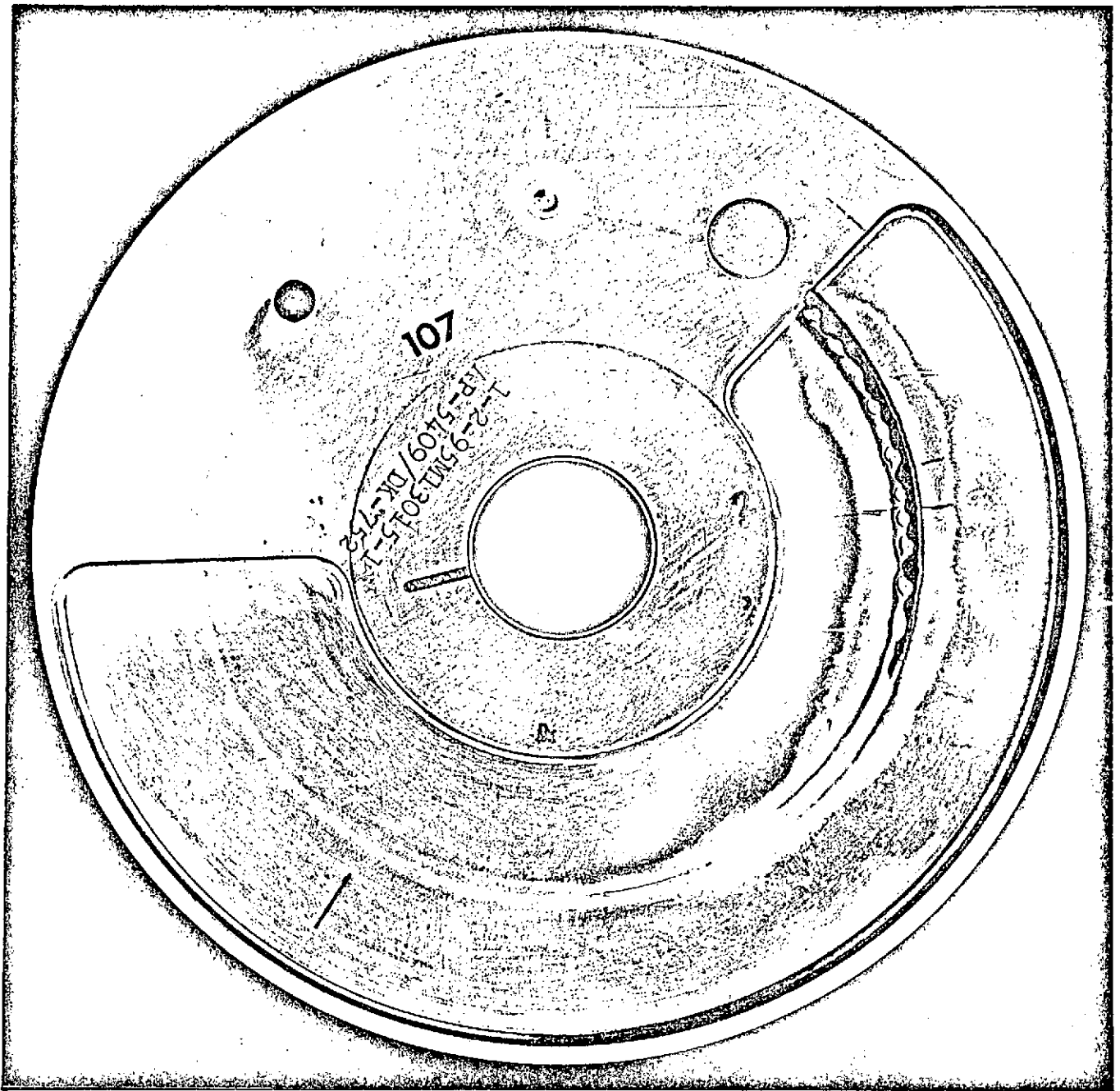


FIGURE A-51. FRONT SURFACE - S/N 107



7G510-1X

FIGURE A-52. BACK SURFACE

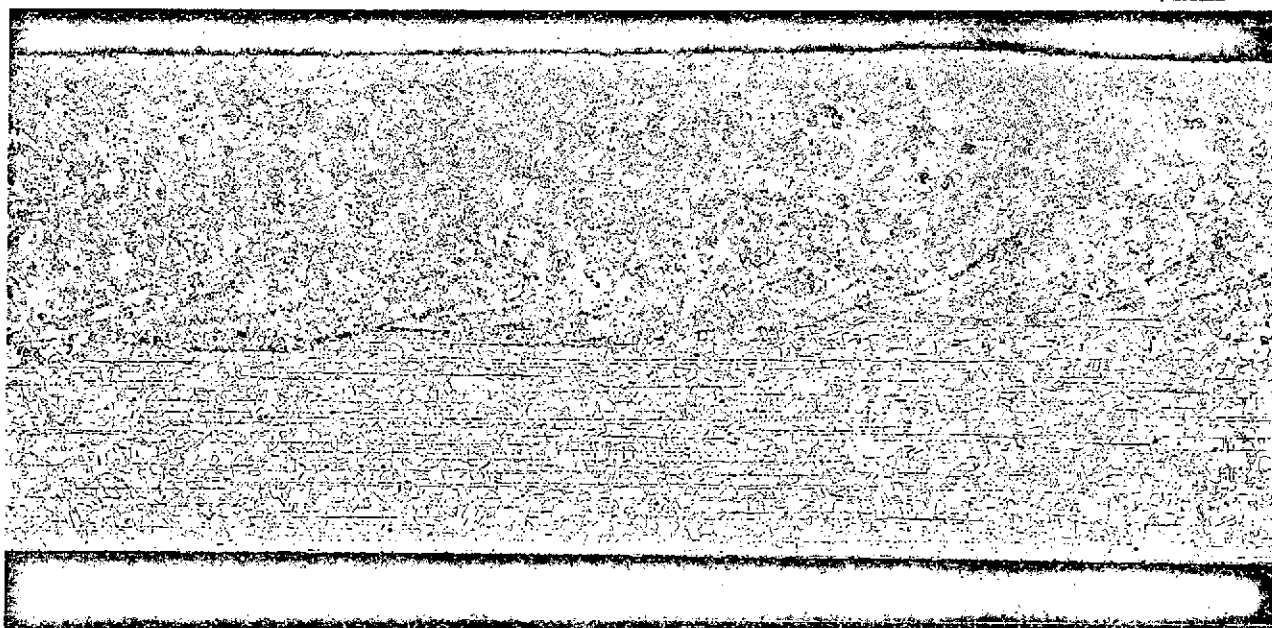


35°(*)

Etched

7G522-20X

FIGURE A-53. SECTION THROUGH CUT REGION
S/N 107

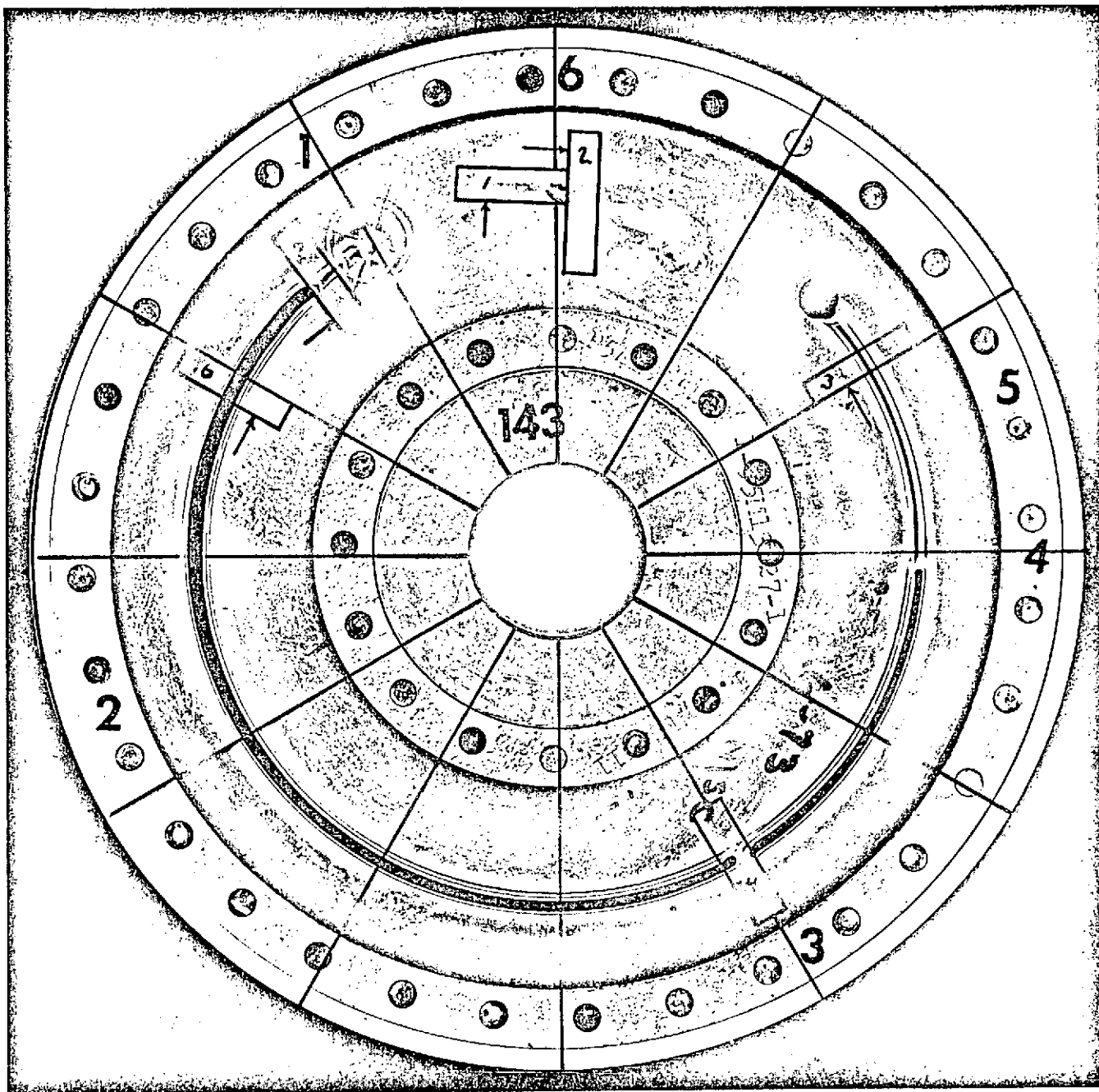


160°-180°

Etched

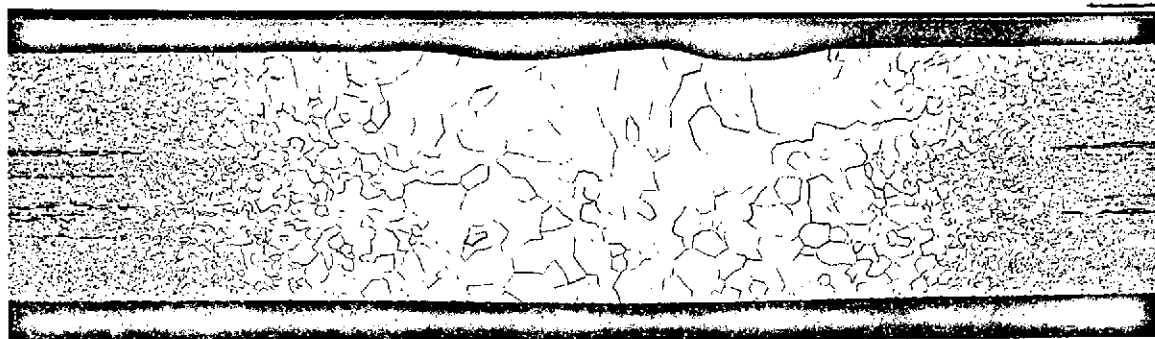
7G521-20X

FIGURE A-54. CHORD SECTION THROUGH FULL
PENETRATION REGION - S/N 107



5G444-1X

FIGURE A-55. FRONT SURFACE - S/N 143



15°(-)

Etched

7G509-20X

FIGURE A-56. SECTION THROUGH REGION BEFORE CUT S/N 143



35°(-)

Etched

7G506-20X

FIGURE A-57. SECTION THROUGH CUT REGION S/N 143

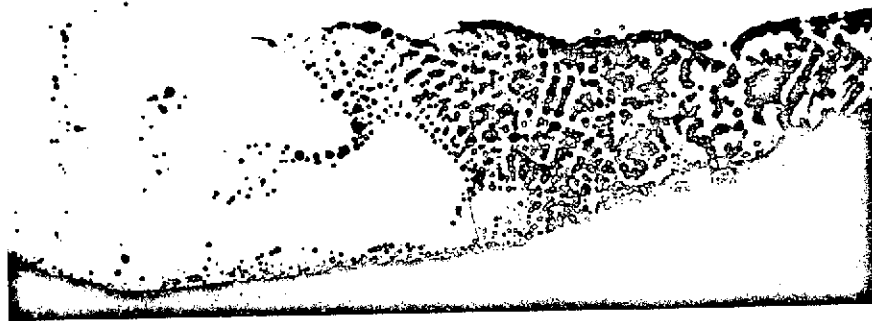


350°(-)

Etched

7G507-100X

FIGURE A-58. BOTTOM SURFACE OF OUTSIDE CUT EDGE S/N 143

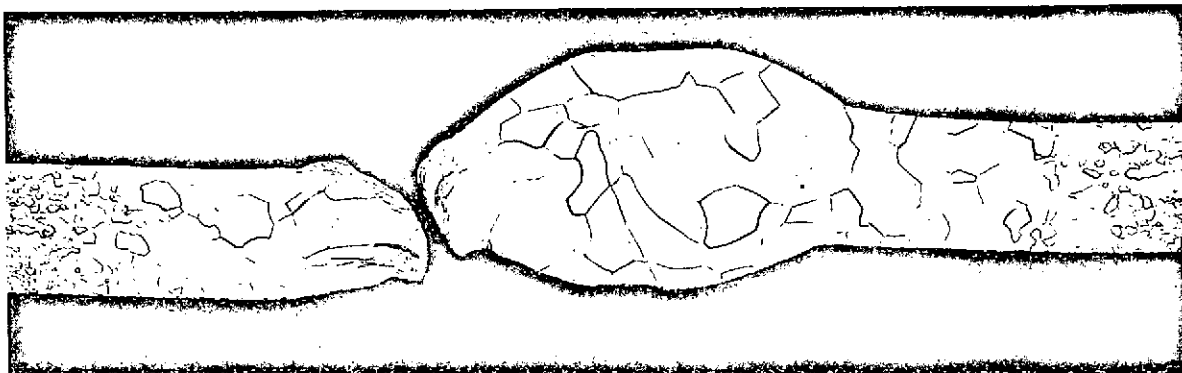


35°(-)

Etched

7G508-250X

FIGURE A-59. BOTTOM SURFACE OF INSIDE
CUT EDGE S/N 143



175°(+)

Etched

7G504-20X

FIGURE A-60. SECTION THROUGH BRIDGE BROKEN
IN CUTTING S/N 143



270°(+)

Etched

7G503-20X

FIGURE A-61. SECTION THROUGH PARTIAL PENETRATION
REGION S/N 143

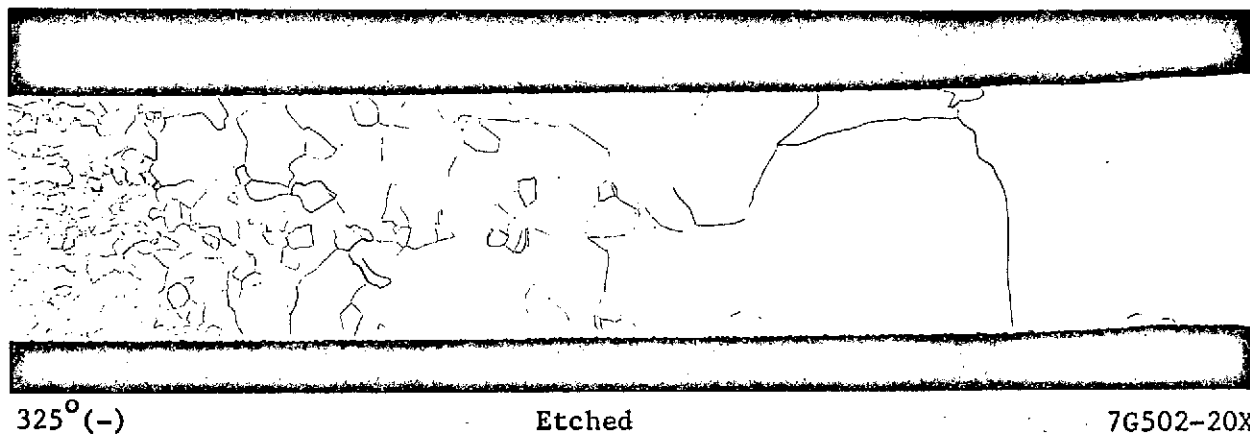


FIGURE A-62. SECTION THROUGH DWELL REGION
S/N 143

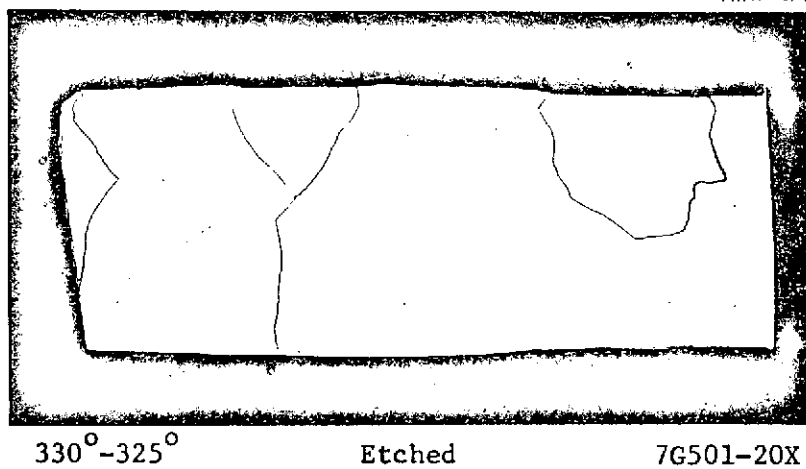
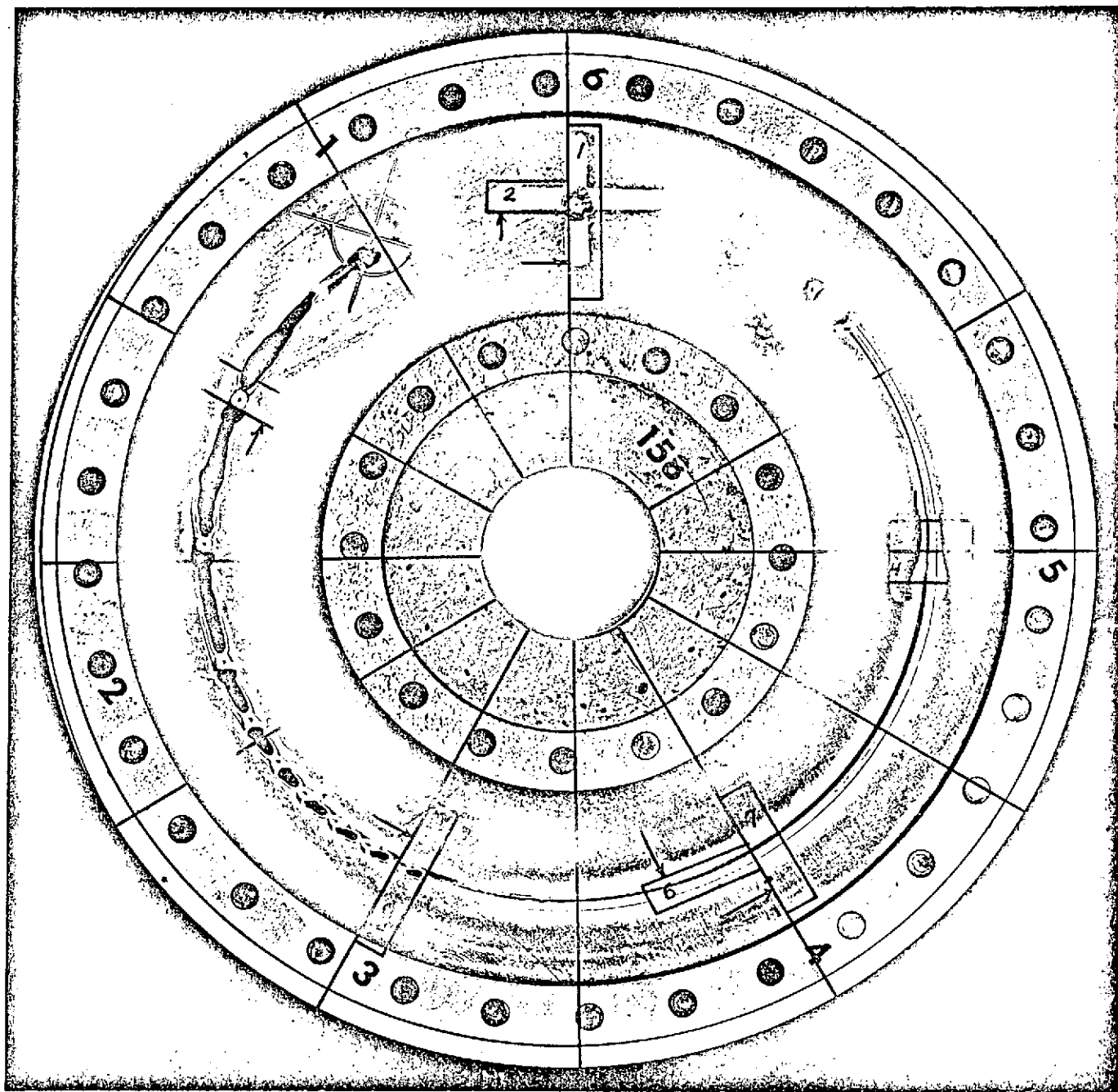
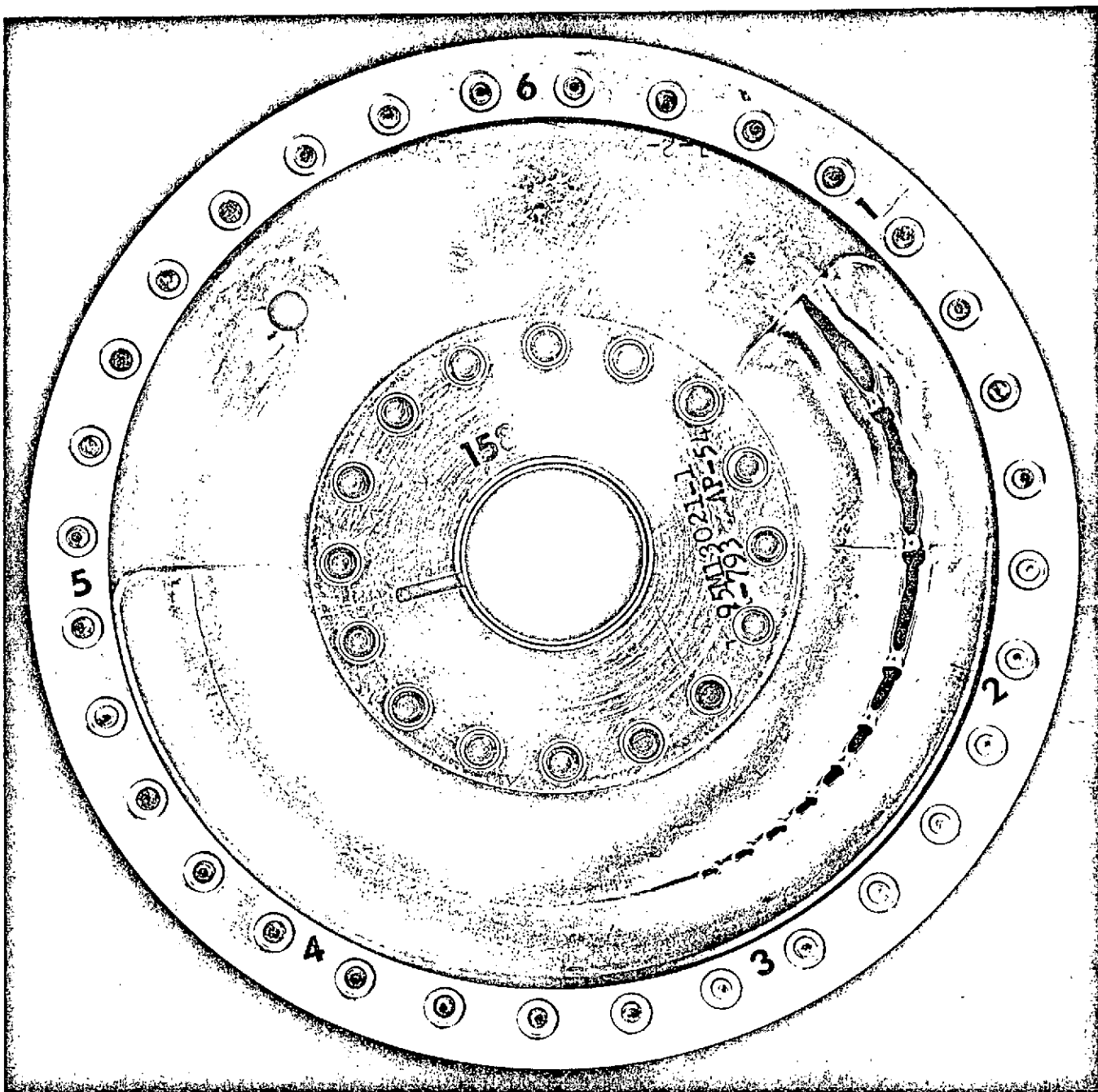


FIGURE A-63. CHORD SECTION
THROUGH DWELL
REGION S/N 143



7G515-1X

FIGURE A-64. . FRONT SURFACE S/N 158



7G514-1X

FIGURE A-65. BACK SURFACE S/N 158

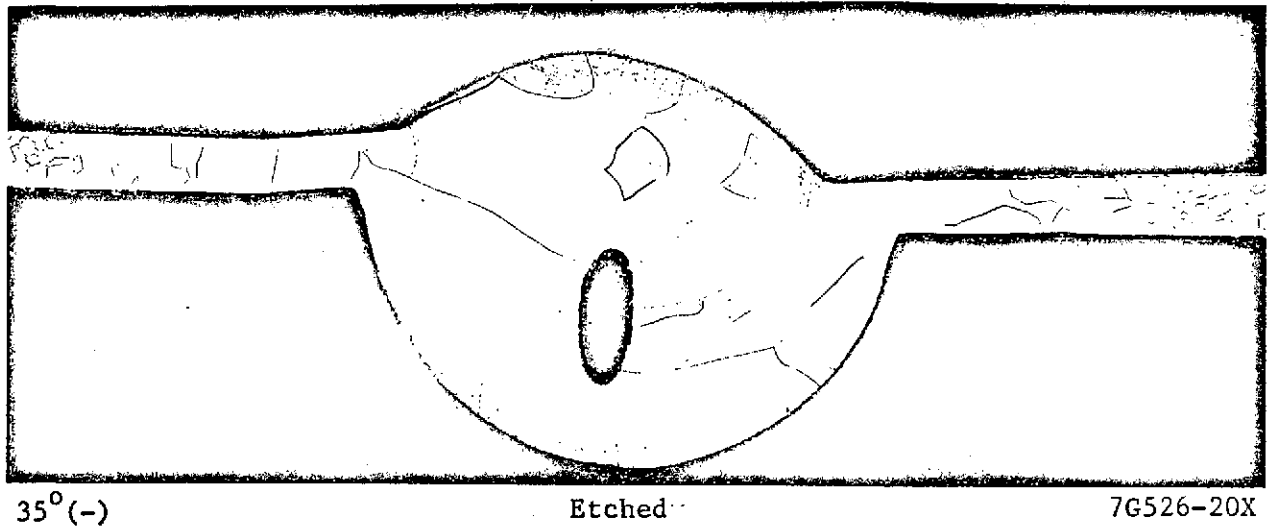


FIGURE A-66. SECTION THROUGH BRIDGE IN CUT REGION S/N 158

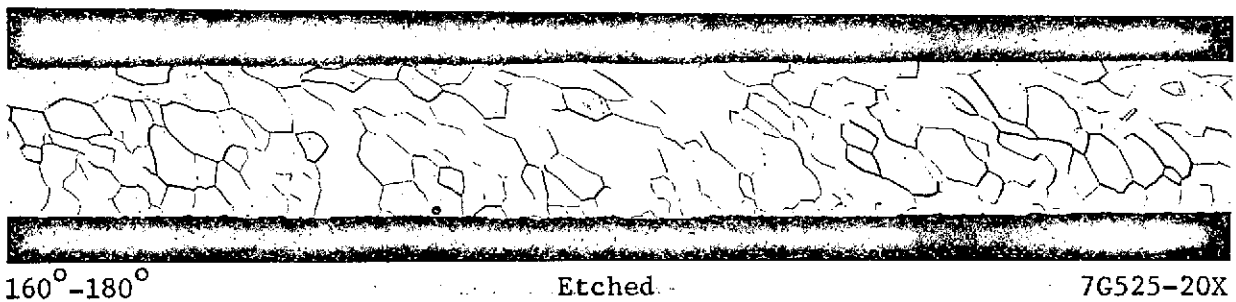


FIGURE A-67. CHORD SECTION THROUGH FULL PENETRATION REGION S/N 158

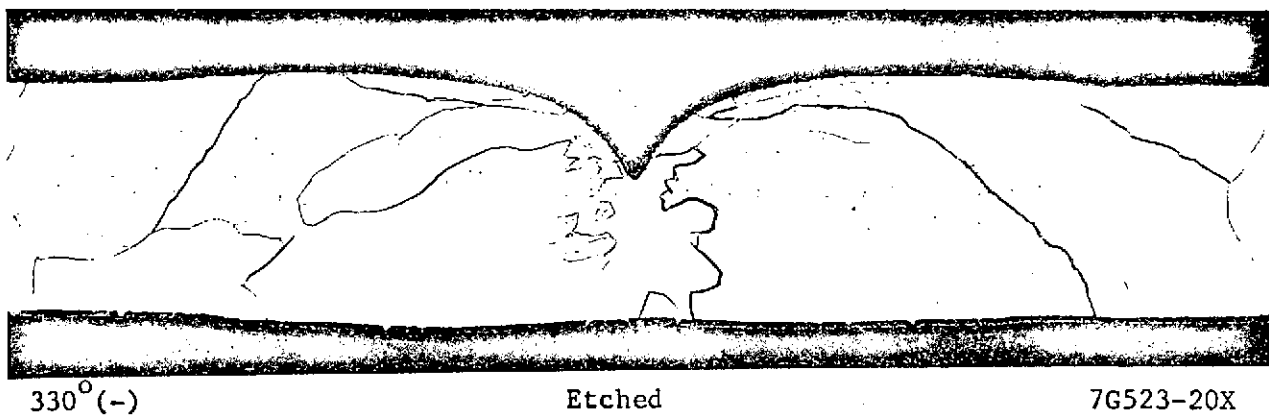


FIGURE A-68. SECTION THROUGH DWELL REGION S/N 158

TABLE A-1. DISTORTION MEASUREMENTS

Location, degrees	Distortion, inch x 10 ⁻³ (a)					
	Aluminum S/N 132		Stainless Steel S/N 107		Tantalum S/N 158	
	In	Out	In	Out	In	Out
0	-2	-2	0	+3	0	+1
30	-2	-23	+5	+6	+2	+2
60	+3	-32	+8	+16	0	0
90	(b)	-28	+5	+11	0	0
120	+1	-13	+2	+2	0	0
150	+1	-1	+2	+4	0	+2
180	+4	+4	+1	+4	0	+2
210	+2	-1	-1	+4	0	0
240	0	-8	-2	+4	0	0
270	-3	-11	-1	+4	0	0
300	-4	-8	+1	+3	+1	0
330	(b)	(b)	0	+3	0	+1

(a) + = distortion toward electron gun

- = distortion away from electron gun

(b) No measurement, probe in cut or dwell region.